CHNICAL REPORT STANDARD TITLE PAGE

1. Report No.	2. Government Accession No.	3. Recipient's Catalog No.
FHWA/AZ-84/194-I		

4. Title and Subtitle	5. Report Date
STATIC AND DYNAMIC BEHAVIOR OF MONOTUBE SPAN-TYPE SIGN STRUCTURES Volume I - Final Report	May, 1984 6. Performing Organization Code

7. Author(s)	8. Performing Organization Report No.
M. R. Ehsani, S. K. Chakrabarti and R. Bjorhovde	

9. Performing Organization Name and Address	10. Work Unit No.
Arizona Transportation and Traffic Institute College of Engineering University of Arizona Tucson, Arizona 85721	11. Contract or Grant No. HPR-1-23(194)
12. Sponsoring Agency Name and Address Arizona Transportation Research Center Arizona Department of Transportation Arizona State University Tempe, Arizona 85281	13. Type of Report and Period Covered FINAL June 83 - May 84 14. Sponsoring Agency Code

15. Supplementary Notes Prepared in cooperation with the U.S. Department of Transportation, Federal Highway Administration, from a study of Monotube Span-Type Sign Structures. The opinions and conclusions are those of the authors and not necessarily of the Federal Highway Administration.

16. Abstract

The report presents the results of the first major investigation into the static and dynamic behavior characteristics of monotube span-type sign structures. Detailed static and dynamic stresses and deflections have been determined for an actual 100 ft span sign structure, utilizing 2- and 3-dimensional finite element modeling. Parametric studies have also been made, where the effects of column stiffness, beam stiffness, span, and sign location and size were examined. It is shown that in-plane and out-of-plane analyses can be conducted independently, and that stresses for tubular members can be determined by vector addition. Static in-plane deflections generally govern the design, but do not satisfy the current AASHTO requirement of $d^2/400$, where d=depth of sign in feet. Structural resonance is found for a very narrow range of wind speeds, assuming no damping and sustained wind over a prolonged period. Design recommendations are made on the basis of stress and deflection computations for simple planar frames. Cambering is recommended for structures where gravity load deflections may be aesthetically undesirable.

Volume II - Appendices, 61 pages

17. Key Words	18. Distribution Statement
Monotube; sign structures; single span; behavior; static; dynamic; stresses; deflections; design criteria; evaluating criteria.	No restrictions. This document is available to the public through the National Technical Information Service, Springfield, VA 22161.

19. Security Classif. (of this report)	20. Security Classif. (of this page)	21. No. of Pages	22. Price
Unclassified	Unclassified	105	

Form DOT F 1700.7 (8-69)

ACKNOWLEDGMENTS

The investigation described in this report was funded by the Arizona Department of Transportation in cooperation with the Federal Highway Administration under Project No. HPR-1-23 (194).

The authors would like to thank Dr. R. H. Wortman and R. A. Jimenez of the Department of Civil Engineering at the University of Arizona. Dr. Wortman was of significant help during the initial stages of the project, and Dr. Jimenez assisted in the administration of the project as the Director of the Arizona Transportation and Traffic Institute.

The continuous support and helpful suggestions of the Arizona Department of Transportation personnel, in particular Messrs. Frank R. McCullagh, Roger Hatton, Rudolf Kolaja, Jamal Sarsam, James Pyne, and Mike Sarsam are gratefully acknowledged.

The cooperation and hospitality of Valmont Industries, Inc. and especially those of Mr. Tom Sanderson during the visit to their manufacturing facilities located at Valley, Nebraska are appreciated.

Professor H. A. Kamel of the Department of Aerospace and Mechanical Engineering at the University of Arizona and his associates were helpful in resolving many problems associated with the use of the computer program GIFTS.

Thanks are also due Carole Goodman, who did an excellent job in typing the report.

TABLE OF CONTENTS
VOLUME I

LIST OF FIGURES
VOLUME I

LIST OF TABLES
VOLUME I

TABLE OF CONTENTS
VOLUME II

LIST OF FIGURES
VOLUME II

LIST OF FIGURES
VOLUME II

The contents of this report reflect the views of the authors who are responsible for the facts and the accuracy of the data presented herein. The contents do not necessarily reflect the official views or policies of the Arizona Department of Transportation or the Federal Highways Administration. This report does not constitute a standard, specification, or regulation. Trade or manufacturer's names which may appear herein are cited only because they are considered essential to the objectives of the report. The U. S. Government and the State of Arizona do not endorse products or manufacturers.

1. INTRODUCTION

For many years, truss-type structures have been successfully used to support traffic signs and other implements spanning over the highways. These structures typically consist of two columns supporting a truss or a tri-chord element, which spans accross the width of the road. The traffic signs are fastened to the truss at various locations above the traffic lanes.

The methods of design of highway sign structures are based on the requirements of AASHTO's Standard Specifications for Structural Supports for Highway Signs, Luminaires and Traffic Signals (1), revised in 1978 and 1979, and one of its predecessors, the AASHTO 1968 Specifications for the Design and Construction of Structural Supports for Highway Signs.

The Specifications have guidelines which limit the static deflection of truss span-type structures to an empirical value of $d^2/400$, where d is the depth of the sign in feet. It is clear that this is incomplete at best. For any sign support structure, if the static deflection is found to be excessive, the designer can specify a deeper sign (i.e., larger d), and thus satisfy the code requirements. In brief, the current AASHTO guidelines are for the most part limited to a requirement that the design be based on rational engineering judgment and principles.

Although the performance of the truss structures in general has been satisfactory, they are expensive to fabricate and, in most cases, the application of the deflection criterion has resulted in structures which are not economical, compared to the available pre-engineered structures. Therefore, due to the growing number of needed sign support structures, the trend has been shifting toward the use of monotube structures which are more economical and aesthetically pleasing.

The monotube structures consist of linearly tapered steel tubes with a constant wall thickness. Figure 1.1 shows a typical monotube sign support structure. As indicated in this figure, the columns are a one-piece tapered member with a larger cross section at the base. The beam consists of two tapered elements, connected such that the largest cross section is at the middle of the span. The beams are attached to the top of the columns by a simple connection, such as the one shown in Figure 1.2. Figure 1.3 shows a drawing of a monotube structure with the details of the connection of the beam elements at the midspan.

The Specifications do not address the design of monotube structures adequately and, in the case of cantilever structures in particular, the design is based entirely on "engineering judgment". In addition, there

Fig. 1.1 Typical Monotube Sign-Support Structure (Courtesy of Valmont Industries, Inc., Valley, Nebraska)

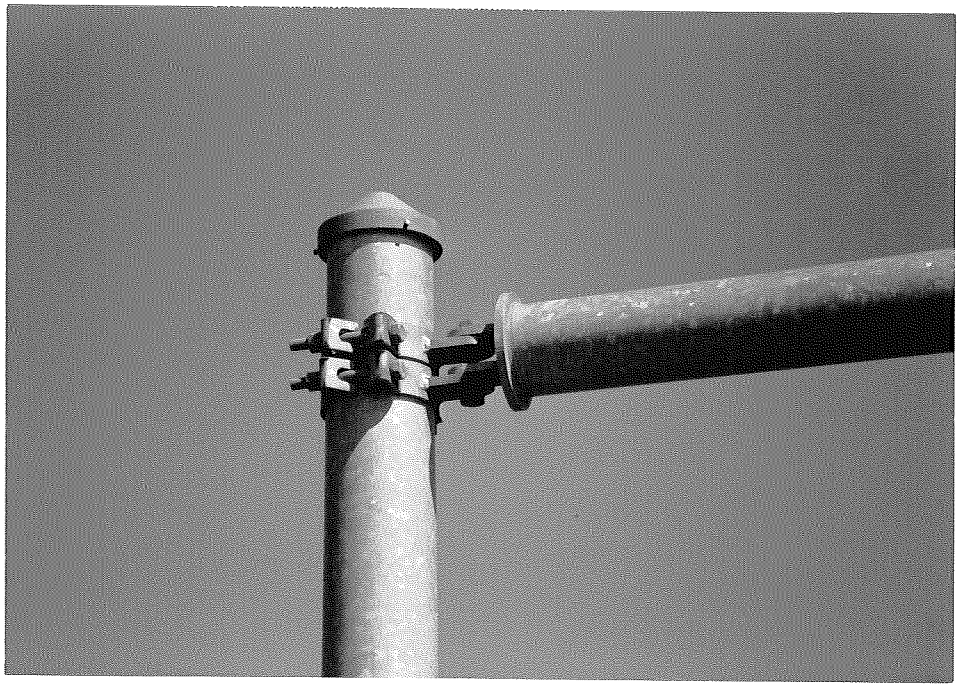

Fig. 1.2 Beam to Column Connection for a Sign-Support Structure (Courtesy of Valmont Industries, Inc., Valley, Nebraska)

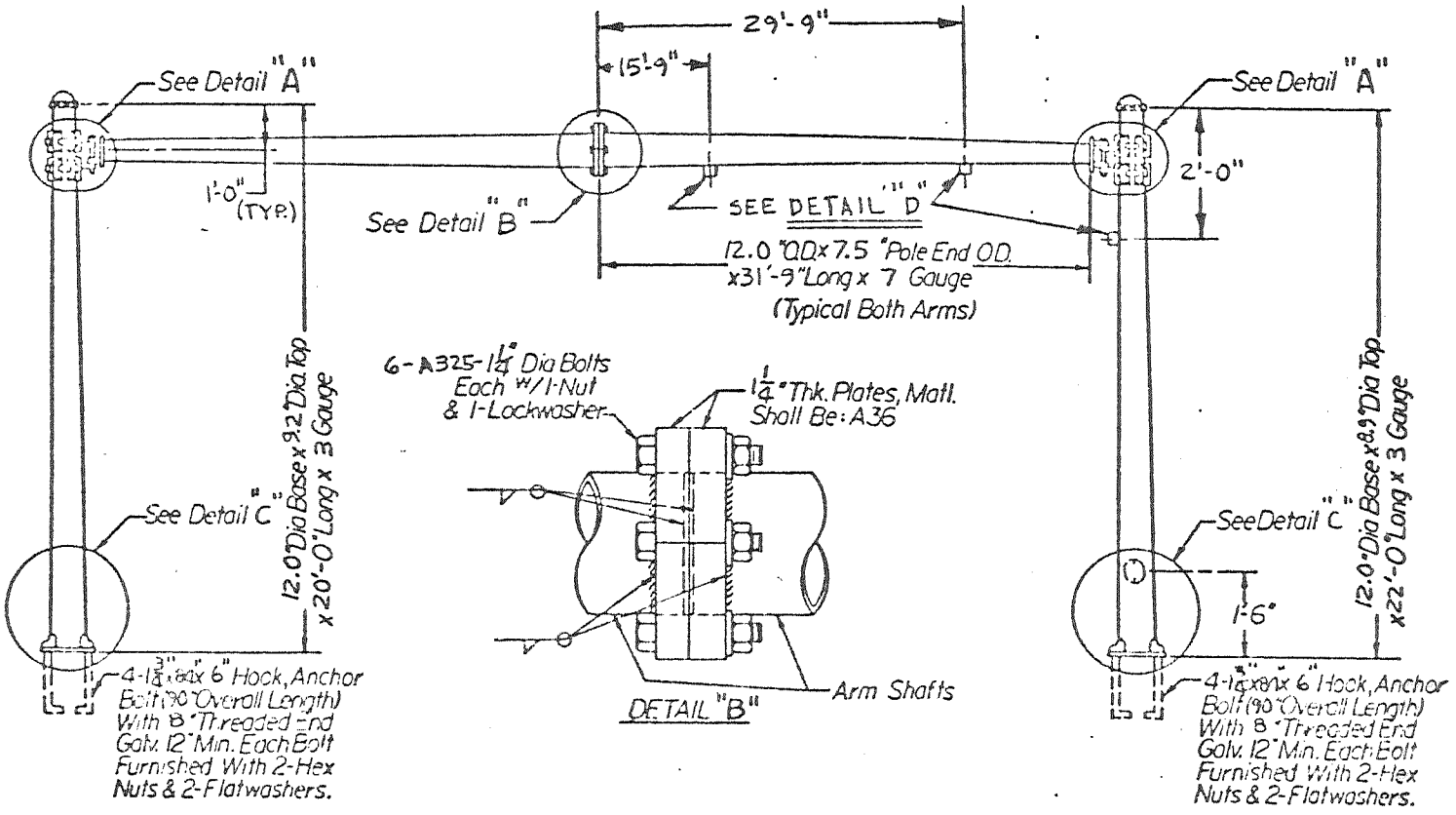

Fig. 1.3 Drawing of Monotube Structure (Courtesy of Valmont Industries, Inc., Valley, Nebraska)

are no guidelines for the design of structures supporting luminaires and traffic signals.

The lack of detailed and adequate design criteria can partly be attributed to a sparsity of research and engineering data on the behavior and strength of such structures. This is due to the complexity of the topic, which involves a need for an understanding of the response of the structure to wind loads (i.e., aerodynamic behavior of a light-weight structure), the influence of material types and cross sectional shapes of the monotubes, and the long-term service characteristics of the structure. The latter subject addresses the question of fatigue as well as the uses and re-uses of the structures. In particular, it is common practice to move a sign from one location to another, thereby changing the service conditions of the structure significantly. It is not known to what degree this form of usage changes the operating characteristics of the sign structure; conjecture can estimate that the cumulative effect of fatigue damage, for example, may be substantial.

The manufacturers of monotube structures, each having their own design procedures, produce such structures using sections which vary considerably both in material as well as cross sectional properties. As a result of this, the transportation authorities are faced with the problem of "accepting" or "rejecting" different designs without any rational guidelines to rely upon.

2. SCOPE AND OBJECTIVES

The primary objective of this study is to develop an appropriate analytical model which will enable the design engineers to provide a rational evaluation of the performance of monotube sign support structures. The study is limited to structures for which the beam elements are supported at both ends. Therefore, cantilever-type structures are excluded from consideration.

The effects of static and dynamic loading of the structures due to gravity and wind loads are examined in detail. Although in some cases fatigue may govern the behavior problems of this kind are not addressed in this study due to time limitations.

The scope of the study is given by the following five categories:

1. Survey and Review of Existing Structures and Design Methods

   a. Types of structures and materials.
   b. Fabrication practices.
   c. Design practices and criteria (e.g., which design specifications are used).
   d. Literature dealing with related structures and their strength and behavior.
   e. Any special subjects (e.g., unique base details, etc.).

2. Evaluation of Current Methods

   Evaluate current design philosophies and criteria, and compare them with existing specifications, such as AISC and AISI.

3. Development of Analytical Model

   Develop analytical model for the support structure with consideration of:

   a. Structural strength, including material and similar criteria.
   b. Stiffness (deflection).
   c. Dynamic characteristics, including thoe of the wind load and the response of the structure.

4. Model Evaluation

   Evaluation of model performance and comparison with current design methods.

5. Development of Design Criteria

Develop new design criteria, in light of findings in Sections (2), (3) and (4).

3. PREVIOUS AND RELATED STUDIES

Over the past fifteen years, a number of studies have been carried out dealing with the behavior of sign support structures. Each of these investigations concentrated on a certain aspect of the problem, which, although helpful in formulating the analysis of monotube structures, do not directly address the behavior of monotube sign support structures.

A few studies have examined the effects of wind on the structures, and the measurement of such parameters as the drag coefficient for different cross sections (2, 3, 4, 5, 6). Hay (4) compared the results of wind tunnel tests with field measurements on a full-scale sign gantry, and developed simple guidelines for approximating the wind forces on these structures. Zell (5) instrumented two sign support structures under service conditions, and concluded that for a typical structure, vehicle-induced gust loads do not appreciably reduce the life expectancy of the structure. Fung (6) provided a complete treatment of the determination of the forcing function as a result of vortex shedding, and the relationship between the wind speed and the vortex shedding frequency. A detailed discussion of this subject is presented in Chapter 5.

Studies have also been carried out on the structural properties and the feasibility of utilizing different materials in the construction of sign support structures. Although limited information is available which deals directly with sign support structures (7, 8), there are several references which address the design of structures made with tubular sections (9, 10, 11, 12). The work of Sherman (9) in producing design criteria for such nenbers, and the study to develop a design guide for outdoor advertising signs (10) are of significance. Similarly, the design specifications of the American Institute of Steel Construction (AISC) (11), and the American Iron and Steel Institute (AISI) (12) offer design criteria that are of direct use. There are otherwise available a number of papers and reports dealing with the behavior of tubular members; the lists of references given in the Commentary of Reference (10) are important in this respect.

A number of studies have dealt with the behavior of different types of structures subjected to wind, such as the work on wind-induced vibrations in antenna members by Weaver (13). However, the majority of the related studies deal with truss-type or tri-chord sign support structures (14, 15, 16). Kumar, et al. (14) analyzed two tri-chord structures subject to different wind velocities. They considered the vortex-shedding excitation of the structures under moderate wind velocities and the drag forces under severe gusts. Although they did recommend design procedures for truss-type structures, their main effort dealt with the evaluation of the Stockbridge damper to reduce the maximum displacement of the structure under vortex-shedding conditions.

Pelkey (17) studied the behavior of long span monotube structures that had been in place for two or three years, and concluded that for this category of structures, the $d^2/400$ limitation of AASHTO (1) can be relaxed. However, the study was very limited and no specific recommendations were made.

More recently, researchers have been concentrating on the effects of fatigue on these structures. Several studies by the departments of transportation in Kansas and California have either been completed (18, 19, 20, 21) or are currently in progress (22).

It is clear that as far as the monotube sign support structures are concerned, little information is available. However, due to the potential economies of these structures, it is imperative that concise guidelines be developed. This was the ultimate goal of the research work that is presented in this report.

4. STATIC BEHAVIOR OF MONOTUBE STRUCTURES

4.1 Description of Typical Structure

In order to make the study more realistic, it was decided to consider an existing monotube sign support structure as the base model. The Arizona Department of Transportation personnel provided the investigators with the shop drawings for a recently constructed sign support structure. It is located on the west-bound University Drive at the intersection of University Drive and Hohokam Expressway in Phoenix, Arizona.

Details of the dimensions of this structure are shown in Figure 4.1. The structure was designed in accordance with AASHTO Specification for Structural Supports of Highway Signs, Luminaries and Traffic Signals (1). The columns are linearly tapered circular tubes, with the largest diameter at the base of the column. Due to the site topography, the columns were constructed in different lengths in order to obtain the same elevation at the top of the columns. The beam is 100 feet long and is spliced at the approximate third points, in addition to at the middle of the span. The splices were designed such that the beam had its largest diameter at the midspan and tapered linearly to the ends of the span.

The beam-to-column connection is shown in Figure 4.2. It provides some moment resistance for in-plane bending, and essentially zero resistance for out-of-plane bending. Details of the column-base and the foundation are shown in Figure 4.3. It is reasonable to assume that the column is fully fixed at the base. The location of the traffic signs can be seen in Figure 4.1, and a typical sign bracket detail is illustrated in Figure 4.4.

4.2 Modeling of the Structure

The structure that is shown in Figure 4.1 was idealized and modeled for a finite element analysis. It was discretized in accordance with the guidelines of the computer program GIFTS (23), which was used in analyzing the structure. A detailed description of the program is given in the next section of the report.

The entire frame was discretized as an assembly of thirty beam elements, as shown in Figure 4.5. In order to analyze the frame in three-dimensional (3-D) space, each beam element was allowed to have three translational degrees of freedom at each node (i.e., displacements in the x, y and z directions) as well as three rotational degrees of freedom at each node (i.e., rotations about the x, y and z axes). The x, y and z axes, as indicated in Figure 4.5, are considered to be the global axes for the finite element analysis.

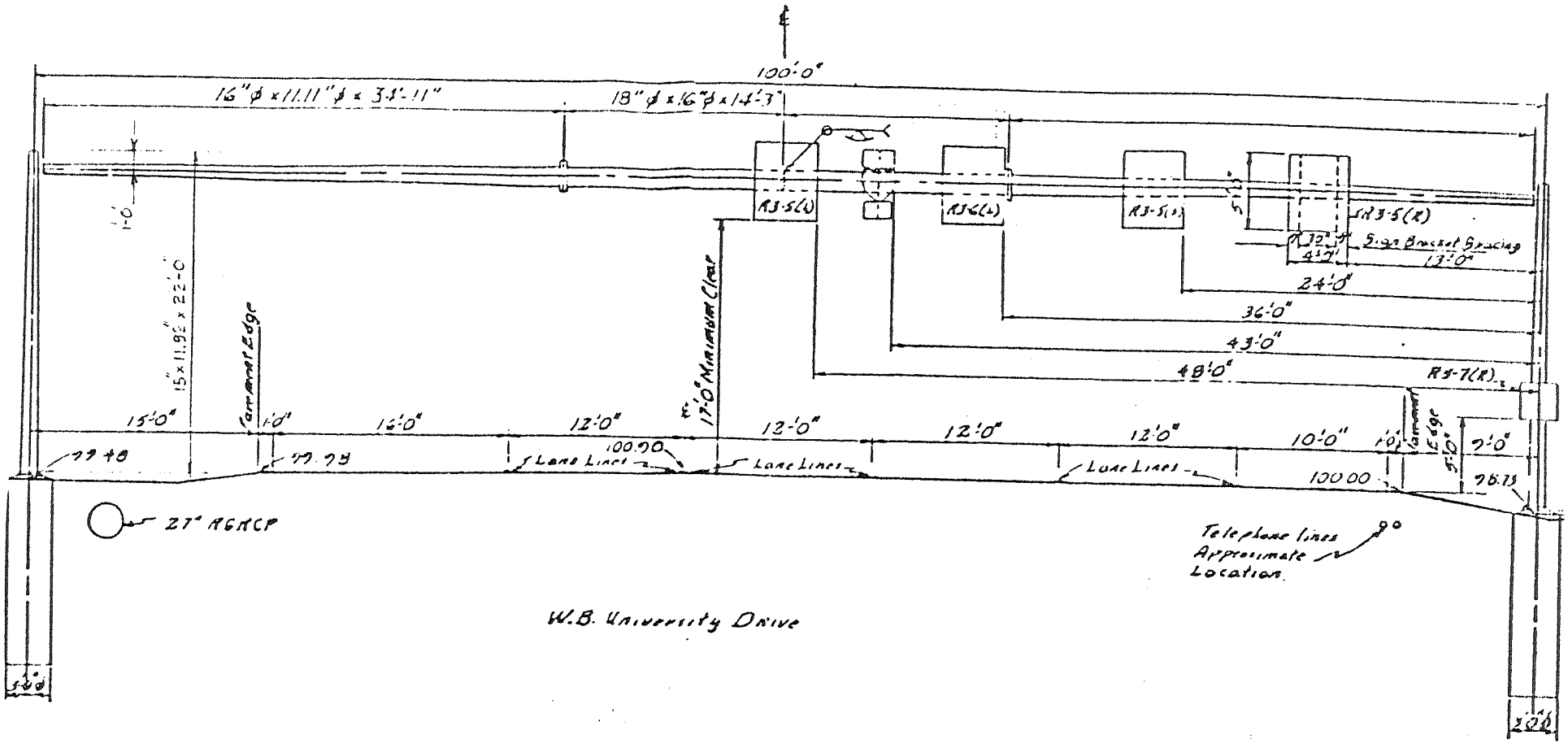

Fig. 4.1 Monotube Structure Used as Base Model for Study

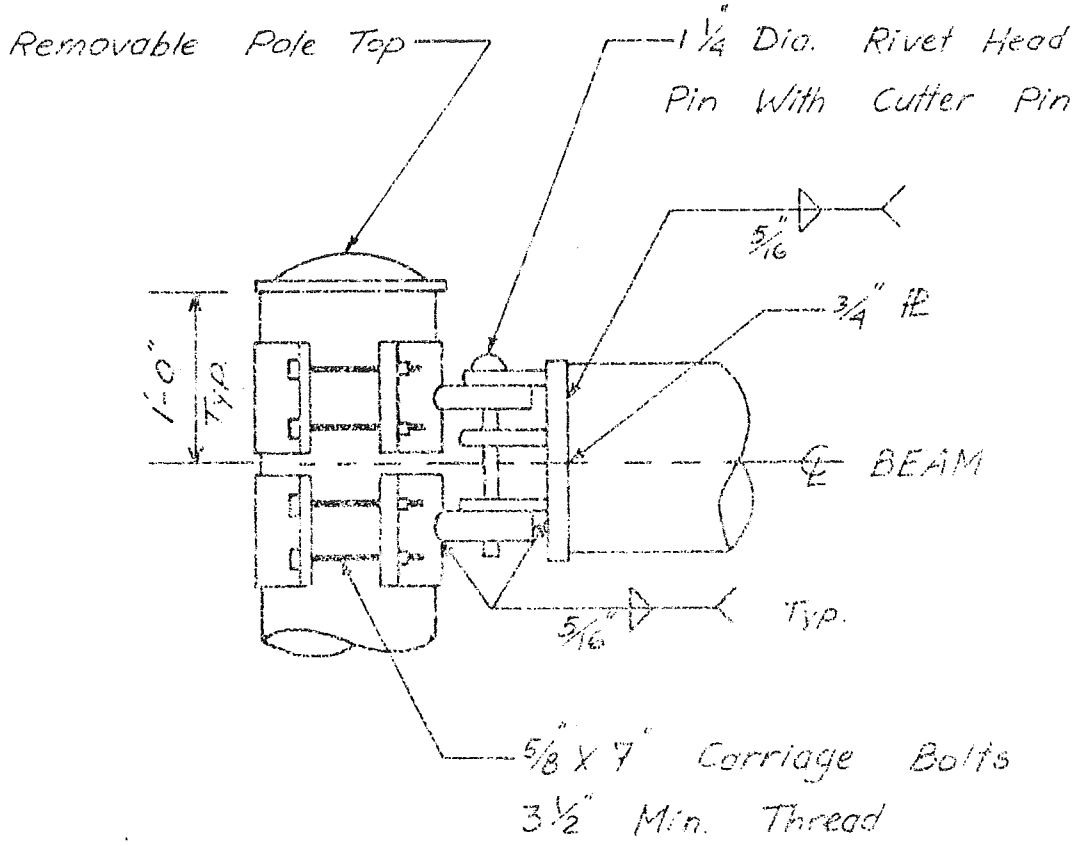

BEAM CLAMP DETAIL

Fig. 4.2 Typical Beam-to-Column Connection

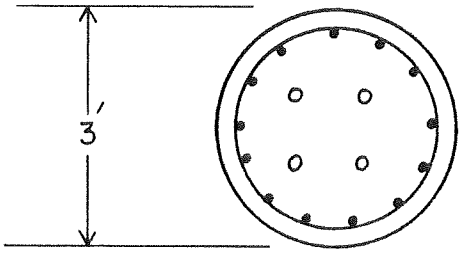

SECTION A–A

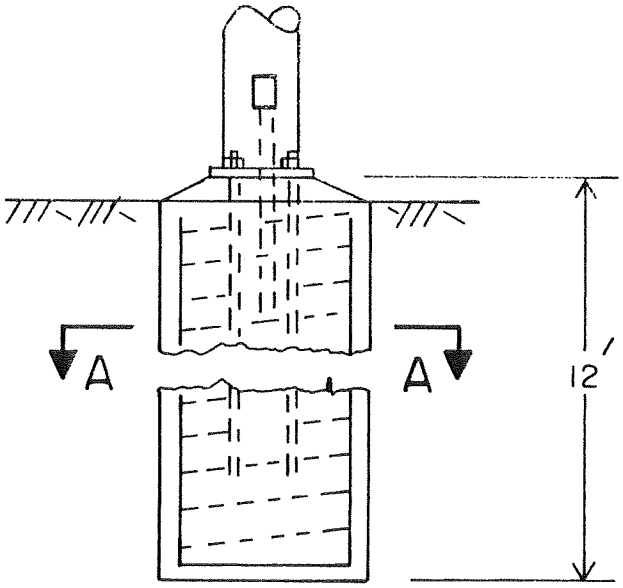

ELEVATION

Fig. 4.3 Typical Base Detail for Monotube Structure

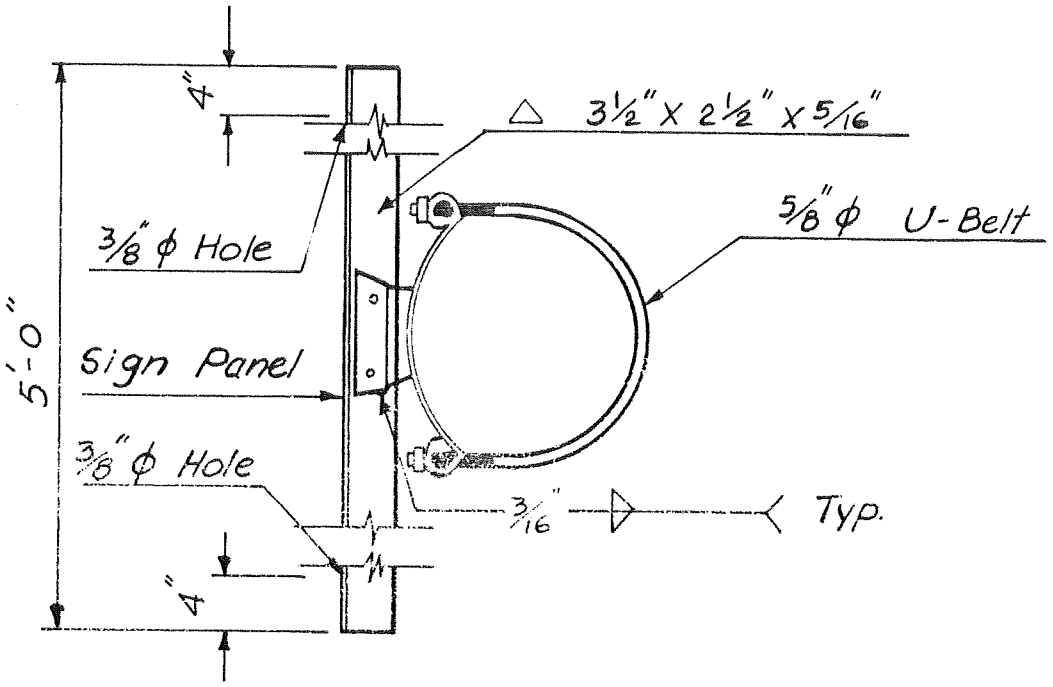

SIGN BRACKET
(Without Sign Light)

Fig. 4.4 Detail of Traffic Sign Support Bracket

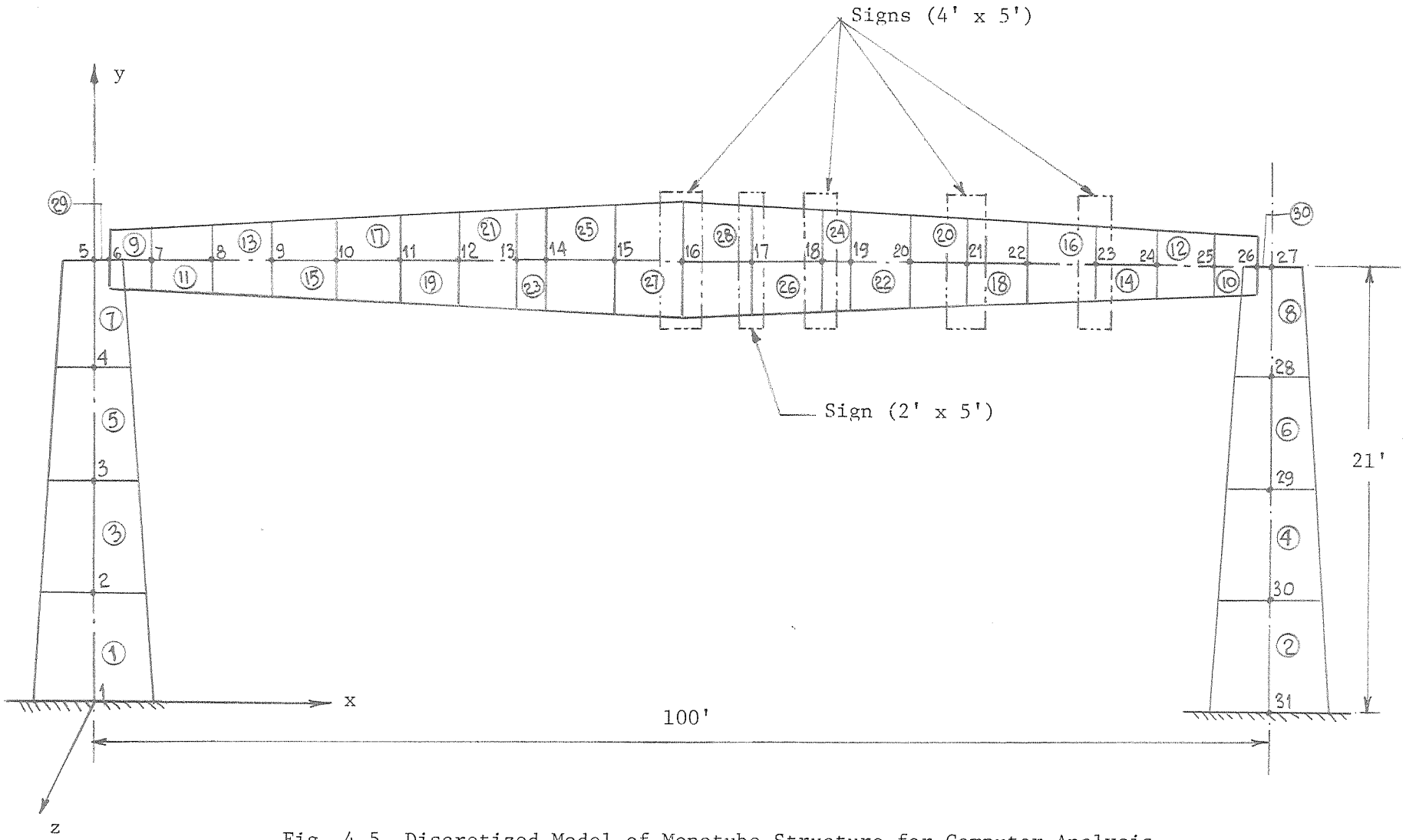

Fig. 4.5 Discretized Model of Monotube Structure for Computer Analysis

The program cannot accept elements with a varying cross section such as that of the tapered members used in monotube structures. Based on this limitation, the structure was modeled with a number of elements where the cross section of each was assumed to be constant and equal to the average of the cross sections at the two ends of that element. It is noted that, considering the large number of elements used for the analysis, this simplification will not result in any appreciable error. The wall thickness of the tubes was taken as 3/16-inch, which was the specified minimum wall thickness on the shop drawings.

The column base was considered to be fully fixed against all translational and rotational degrees of freedom. The beam splices shown in Figure 4.6 were assumed to provide full continuity between the adjoining members.

The most complicated element to model was the beam-to-column connection. The capacity of the connection in transferring shear forces depends on its cross sectional area, while its capacity in transferring bending moments is proportional to the moment of inertia. It was decided to model the connection as a short beam, having a rectangular cross section. The cross sectional area of the actual connection was used as the cross sectional area for the connection model. This assured comparable behavior in shear between the real connection and the connection model. Because the actual connection has almost no resistance in bending about the y-axis (out-of-plane), the connection rectangle had its longer side along the y-axis, as shown in Figure 4.7. The ratio of the dimensions of the rectangular connection model and its length along the x-axis was selected such that the z-axis bending stiffness of the actual connection and the model were approximately the same.

In selecting the elements for the beam, a node was always assumed at the centroid of each of the traffic signs, such as nodes number 16, 17, 18, 21 and 23 in Figure 4.5. It was assumed that the signs were connected to the beam at these points, and therefore the weight of the signs would be applied to the beam at these nodes.

4.3 Computer Program

After investigating a number of alternatives, it was decided to use the computer program GIFTS (Graphics-Oriented Interactive Finite Element Analysis Time-Sharing System) (23) for the analysis of the structure. This program, which has been developed at the University of Arizona, is a finite element pre- and post-processing and analysis package which may be implemented and run on a variety of minicomputers and time-sharing systems. It may be used with a graphics terminal, usually a storage tube device, or with an ordinary alphanumeric terminal. For this study,

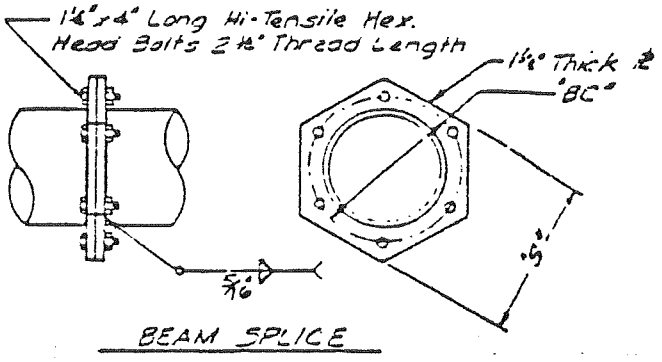

BEAM SPLICE DATA				
* Beam Size Thickness	Dia	"BC"	"S"	"T"
3/16"	16"	19"	20¼"	1⅛"

* Minimum

Fig. 4.6 Typical Beam Splice Detail for Monotube Structure

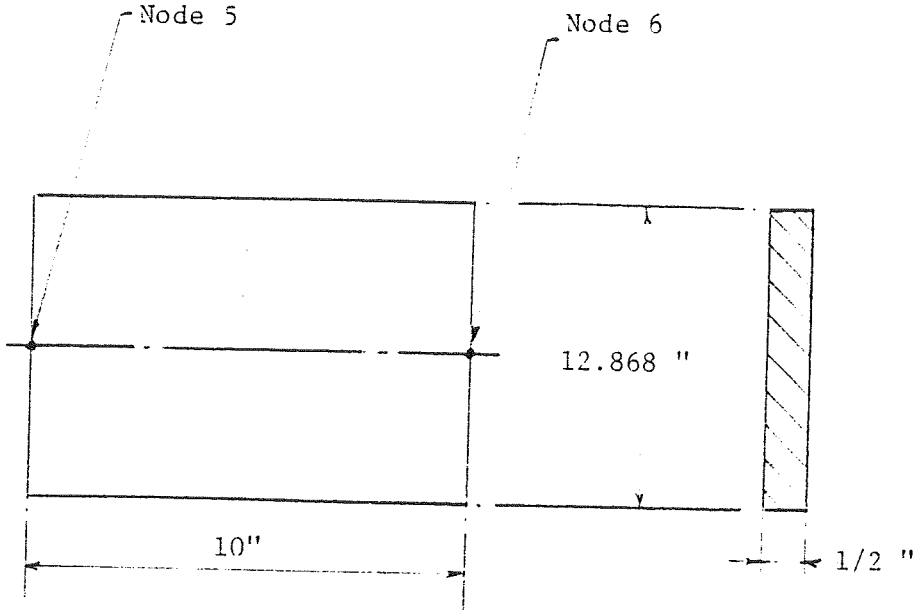

Fig. 4.7 Details of Beam-to-Column Connection Element for FEM Modeling

the program was run on the Data General Eclipse S-230 computer in the Department of Aerospace and Mechanical Engineering at the University of Arizona.

GIFTS is not a single program, but rather a group of fully compatible programs (modules), constituting a program library. Each module can be used for a specific function, such as stiffness matrix computation and assembly, or for a class of operations, such as load and boundary condition generation. GIFTS can handle different loads and loading cases on the structure, subjected to given boundary conditions for computation of stresses and deflections at all nodal points.

4.4 Loads on the Structure

The structure was analyzed for the static loads resulting from the self weight of the structure, ice loads, and wind pressure. A more detailed description of each loading case is given below.

4.4.1 Dead load. The weight of each element was calculated assuming a specific weight of 490 pounds per cubic foot for steel. The weight of each element was then equally divided between the two end nodes. The weights of the signs were calculated assuming that they weigh 10 pounds per square foot of surface area. These weights were assumed to act on the structure at the nodes where the beams support the signs, as discussed in Section 4.2. The nodal loads due to the dead load of the structure are listed in Table 4.1.

4.4.2 Ice load. In accordance with the Specifications (1), ice loads of 3 pounds per square foot of the actual area of the structural members and the signs was assumed to act on the structure. The ice loads were also divided among all nodes based on the tributary area of each node. The ice loads acting at each node are given in Table 4.1.

4.4.3 Wind load. Based on Specifications (1), the structure was analyzed for a maximum wind velocity of 70 miles per hour, blowing perpendicular to the plane of the frame, i.e., along the road. The statically equivalent wind loads have been computed as nodal loads, based on the tributary areas of the monotube members and the signs, in accordance with the Specifications (1). Considering the asymmetry of the structure with respect to the location of the traffic signs, the wind loads resulting from the wind blowing in two opposite directions were considered. Wind load (Case 1) corresponds to the wind blowing in the +z direction, and wind load (Case 2) corresponds to the wind blowing in the -z direction. The nodal loads resulting from the wind speed of 70 miles per hour are also listed in Table 4.1.

TABLE 4.1.
STATIC NODAL LOADS FOR DIFFERENT CASES OF LOADING (lbs)

Node No.	Dead Load[1,2]	Ice Load[2]	Wind Load (Case 1)[3]	Wind Load (Case 2)[4]
1	76	30	24.43	24.43
2	148	59	47.62	47.62
3	140	56	51	51
4	132	53	53.4	53.4
5	73	27	28.2	28.2
6	56	20	21.2	21.2
7	107	43	42.82	42.82
8	123	49	49.3	49.3
9	136	54	54.8	54.8
10	151	60	60.6	60.6
11	150	60	60.2	60.2
12	148	59	59.4	59.4
13	112	44	45	45
14	136	54	54.5	54.5
15	205	82	82	82
16	410	204	566.40	566.40
17	305	142	335	335
18	336	174	536.9	536.9
19	112	44	45	45
20	148	59	59.4	59.4
21	350	180	542.6	542.6
22	151	60	60.6	60.6
23	323	174	537.2	537.2
24	123	49	49.3	49.3
25	107	43	42.82	42.82
26	56	20	21.2	21.2
27	78	27	28.2	28.2
28	132	53	53.4	53.4
29	140	56	51	51
30	148	59	47.62	47.62
31	76	30	24.43	24.43

NOTES:

1. Dead Load includes loads due to the weight of the signs supported at applicable nodes.
2. Dead Loads and Ice Loads are applied in the -y direction (see Fig. 4.5).
3. Wind Load (Case 1) is applied horizontally at each node in the +z direction (see Fig. 4.5).
4. Wind Load (Case 2) is applied horizontally at each node in the -z direction (see Fig. 4.5).

A comprehensive static load analysis of the structure was carried out for which the following six loading combinations were considered:

1. Dead Load
2. Dead Load + Ice Load
3. Dead Load + Wind Load (Case 1)
4. Dead Load + Wind Load (Case 2)
5. Dead Load + Ice Load + Wind Load (Case 1)
6. Dead Load + Ice Load + Wind Load (Case 2)

All of these load combinations are realistic cases for the monotube structures. Due to the relative magnitude of the dead load versus the ice load, for example, the performance of the structure under pure self-weight is important. This applied both to sustained stress levels as well as the question of dead load deflections.

The governing gravity load combination will be No. 2 in the above listing, although ice load is not a realistic criterion in certain geographical areas. The two wind load cases are both valid for design, although Nos. 5 and 6 are extreme cases of combinations (i.e., dead load plus full ice load plus sustained wind of 70 mph). The importance of these will be discussed in detail in Chapter 7. However, it is noted that the allowable stresses for load combinations 3 to 6 are increased by 33-1/3% over those for static design (9, 11, 12).

4.5 Results of the Static Analysis

The static analysis of the structure was carried out for the different loading combinations specified in the previous section of this chapter. The output of the computer program GIFTS for the static analysis consists of the displacements and the stress-resultants for each node in the structure. Although the structure is symmetrical with respect to the overall geometry, member cross sections, column base supports, beam-to-column connections and splices, the asymmetric placement of the signs, which were located only on one-half of the span, as shown in Figure 4.1, results in asymmetrical displacements and stresses. It is noted that in addition to the dead load of the structure, which is affected by the asymmetric placement of the signs, the equivalent wind forces and the loads caused by the formation of ice on the structure also become asymmetric.

4.5.1 Static deflections. The nodal displacements and rotations are given with reference to the global ones x, y and z, and the sign convention for the displacments is shown in Figure 4.8. The deflection components in each of the x, y and z directions are defined as u, v and w, as shown in Figure 4.8. The nodal displacements and rotations for the case of dead plus ice plus wind load are in Table 4.2, as an example

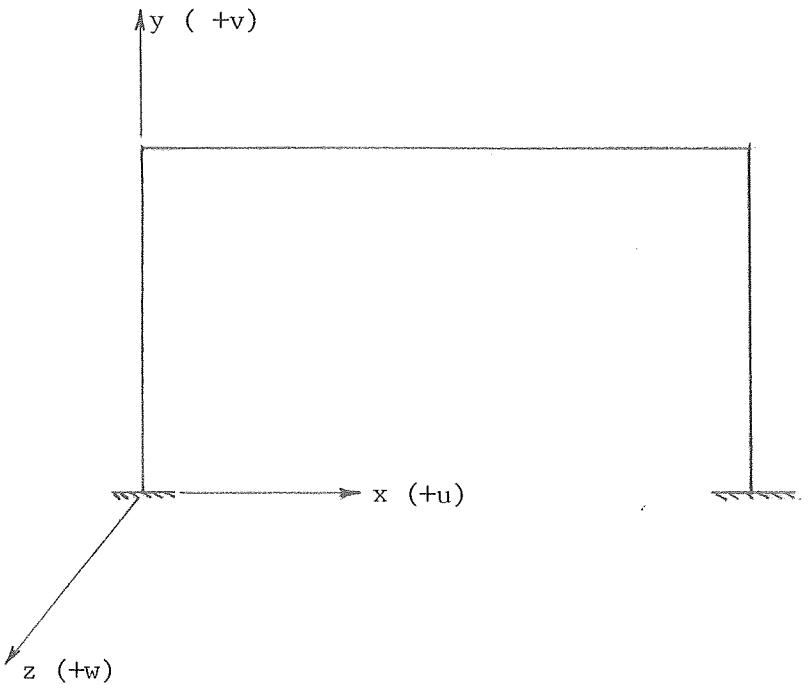

Fig. 4.8 Global and Displacement Coordinates for Monotube Structure

Table 4.2

Static Displacements (in.) and Rotations (rad.)
due to D + I + W(1) Load Combination

Node No.	Displacements (in)			Rotations (rad)		
	u	v	w	θ_x	θ_y	θ_z
1	0.000E-01	0.000E-01	0.000E-01	0.000E-01	0.000E-01	0.000E-01
2	-6.627E-02	-8.004E-04	1.020E-01	3.024E-03	-2.212E-04	1.724E-03
3	-1.923E-01	-1.589E-03	3.783E-01	5.510E-03	-4.799E-04	1.845E-03
4	-2.582E-01	-2.365E-03	7.883E-01	7.245E-03	-7.850E-04	-2.485E-04
5	-9.813E-02	-3.132E-03	1.276E 00	7.936E-03	-1.149E-03	-5.405E-03
6	-9.827E-02	-6.527E-02	1.457E 00	9.811E-03	-2.947E-02	-6.924E-03
7	-9.896E-02	-5.556E-01	2.925E 00	9.834E-03	-2.901E-02	-1.223E-02
8	-9.974E-02	-1.402E 00	4.625E 00	9.858E-03	-2.738E-02	-1.550E-02
9	-1.005E-01	-2.372E 00	6.203E 00	9.879E-03	-2.499E-02	-1.643E-02
10	-1.012E-01	-3.443E 00	7.753E 00	9.897E-03	-2.179E-02	-1.567E-02
11	-1.020E-01	-4.422E 00	9.082E 00	9.913E-03	-1.829E-02	-1.375E-02
12	-1.026E-01	-5.165E 00	1.006E 01	9.925E-03	-1.506E-02	-1.147E-02
13	-1.031E-01	-5.765E 00	1.085E 01	9.936E-03	-1.183E-02	-9.896E-03
14	-1.034E-01	-5.989E 00	1.115E 01	9.940E-03	-1.034E-02	-7.660E-03
15	-1.041E-01	-6.426E 00	1.176E 01	9.951E-03	-6.466E-03	-4.352E-03
16	-1.047E-01	-6.626E 00	1.209E 01	9.960E-03	-2.751E-03	-1.160E-03
17	-1.054E-01	-6.390E 00	1.215E 01	9.969E-03	1.189E-03	2.166E-03
18	-1.060E-01	-6.298E 00	1.190E 01	9.980E-03	5.781E-03	5.899E-03
19	-1.063E-01	-6.118E 00	1.172E 01	9.984E-03	7.655E-03	7.363E-03
20	-1.069E-01	-5.592E 00	1.114E 01	9.994E-03	1.190E-02	1.051E-02
21	-1.075E-01	-4.894E 00	1.031E 01	1.001E-02	1.639E-02	1.351E-02
22	-1.082E-01	-3.890E 00	9.054E 00	1.002E-02	2.155E-02	1.632E-02
23	-1.090E-01	-2.747E 00	7.460E 00	1.004E-02	2.650E-02	1.793E-02
24	-1.097E-01	-1.666E 00	5.743E 00	1.006E-02	3.037E-02	1.760E-02
25	-1.105E-01	-6.847E-01	3.828E 00	1.009E-02	3.301E-02	1.452E-02
26	-1.112E-01	-8.514E-02	2.149E 00	1.011E-02	3.380E-02	8.909E-03
27	-1.113E-01	-3.715E-03	1.928E 00	1.198E-02	1.488E-03	7.259E-03
28	1.470E-01	-2.789E-03	1.191E 00	1.096E-02	1.017E-03	1.515E-03
29	1.454E-01	-1.863E-03	5.713E-01	8.332E-03	6.215E-04	-1.071E-03
30	5.503E-02	-9.345E-04	1.539E-01	4.565E-03	2.865E-04	-1.367E-03
31	0.000E-01	0.000E-01	0.000E-01	0.000E-01	0.000E-01	0.000E-01

of the computer output. Similar results were obtained for all loading cases.

In order to analyze the static deflection results, four significant points on the structure were examined. These are given by nodes number 16, 18, 23 and 27, as shown in Figure 4.5. Point 27 is significant because it defines the top of the column, and node 16 is located at the middle of the span for the beam. It was expected that for most loading cases, the maximum static deflection would occur at this point. Points 18 and 23 were selected to study the variation of the displacements in the beam due to the asymmetric placement of the signs. The static deflections at the four points for the different loading combinations are given in Table 4.3.

It is noted that regardless of the load combination to which the structure was subjected, the static analysis of the structure was always carried out in three-dimensional space. The following conclusions can be made on the basis of the results given in Table 4.3.

(i) In the cases where the wind loads are excluded, such as the load combinations of dead load only and dead load plus ice load, the out-of-plane component of the deflection (i.e., w) is zero. In other words, the displacements of the frame occur entirely in the x-y plane, as expected.

(ii) The out-of-plane deflection of the frame, which is due to the wind load, is not affected by the magnitude of the applied gravity loads which act in the plane of the frame. This is to be expected for the level of gravity load and the type of structure that is being considered. As shown in Table 4.2, the w-component of the deflection is exactly the same for the loading combinations of dead plus wind loads and dead plus ice plus wind loads.

(iii) The in-plane deflection of the frame is not affected by the presence of the wind load. That is, the u- and v-components of the deflection for the loading cases of dead load only or dead load plus wind load are equal. Similarly, the u- and v-components of the deflection for the loading cases of dead plus ice load are identical to those for the case of dead plus ice plus wind load.

(iv) The displacement of the beam is primarily occurring in the plane of and in the same direction as the applied load. As shown in Table 4.3, the u-component of the deflection for points 16, 18 and 23 is at least one order of magnitude smaller than the deflections in the other directions. In other words, effects such as in-plane motion of the column are insignificant.

TABLE 4.3.
STATIC DEFLECTIONS FOR DIFFERENT LOAD COMBINATIONS (inches)

Load Combinations	Node Point	u	v	w
D	16	-0.065	-4.556	0.0
	18	-0.066	-4.320	0.0
	23	-0.068	-1.877	0.0
	27	-0.069	-0.003	0.0
D+I	16	-0.105	-6.626	0.0
	18	-0.106	-6.298	0.0
	23	-0.109	-2.747	0.0
	27	-0.113	-0.004	0.0
D+W(1)	16	-0.065	-4.556	12.090
	18	-0.066	-4.320	11.900
	23	-0.068	-1.877	7.460
	27	-0.069	-0.003	1.928
D+I+W(1)	16	-0.105	-6.626	12.090
	18	-0.106	-6.298	11.900
	23	-0.109	-2.747	7.460
	27	-0.113	-0.004	1.928

(v) The displacement of the top of the column (nodal point 27), primarily occur in the u-direction (in-plane horizontal) when wind forces are not included. This is due to the bending of the beam in the x-y plane, which causes the top of both columns to bend towards the middle of the span. However, when wind loads are considered, the deflection of the columns is primarily in the direction of the wind, i.e., the z-direction.

(vi) The out-of-plane deflection of the beam, i.e., in the z-direction, due to the statically equivalent loads corresponding to a wind velocity of 70 miles per hour is approximately twice the in-plane deflection of the beam due to the combined gravity loads.

Based on parts (i), (ii) and (iii) discussed above, it is concluded that for the service condition for which the structure responds elastically, the displacements from different cases of in-plane and out-of-plane loading can be combined to obtain the final deformed

configuration of the frame. In order to clarify this point, the process of displacement at the midspan of the beam is demonstrated in Figure 4.9. In this figure, the u-component of the deflection has been ignored due to its relatively small magnitude compared to the v- and w-components. Due to the dead plus ice load, point 16 will move 6.626 inches in the negative v-direction (vertically downwards). The equivalent static wind load for a wind speed of 70 mph causes the point to move 12.09 inches horizontally in the direction of the wind, i.e., the +w-direction. Thus, the total displacement of point 16 is equal to the length of the line AA', or

$$\sqrt{(6.626)^2 + (12.090)^2} = 13.78 \text{ in.}$$

An important observation is made with respect to the magnitude of the static deflection of point 16 compared to the allowable $d^2/400$ limit, as required by the current Specification (1). The signs that were attached to the structure that has been used for this study were five feet deep. This leads to an allowable maximum deflection of (5) $d^2/400 = .063$ ft. = 0.75 in. at the midspan of the beam. This is an order of magnitude smaller than the actual maximum static deflection of approximately 4.56 inches (for dead load). It is obvious that considering the stiffness and the span of these structures for a typical situation, the $d^2/400$ limitation cannot be satisfied for monotube single span sign structures.

The large out-of-plane deflection of the beam, discussed in (vi) above, is partly due to the type of the beam-to-column connection that is used, since it does not provide any resistance to bending out-of-plane. It is also noted that this deflection occurs under extreme loading combinations which include that due to a wind speed of 70 mph. As discussed in Chapter 5.4, the equivalent wind loads and the resulting deflections are proportional to the square of the wind speed. Therefore, under a more common wind speed of 20 miles per hour, the out-of-plane deflection of the beam will be approximately $12.09 \cdot (20/70)^2 = 0.99$ inches, which is roughly 1/1200 times the span length. These concepts, as well as the problems of realistic wind speeds and durations, will be discussed in detail in Chapter 6.

4.5.2 Static Stresses. Program GIFTS produces stress resultants at each node in terms of the local axes for that element. These include forces which are given in units of pounds and bending moments which are given in units of inch-pounds. The structure was analyzed for the different loading combinations listed in Section 4.4. The nodal forces for the case of dead plus ice plus wind load are listed in Table 4.4. As far as the analysis of the stress resultants is concerned, two significant points were selected and their stresses studied in detail.

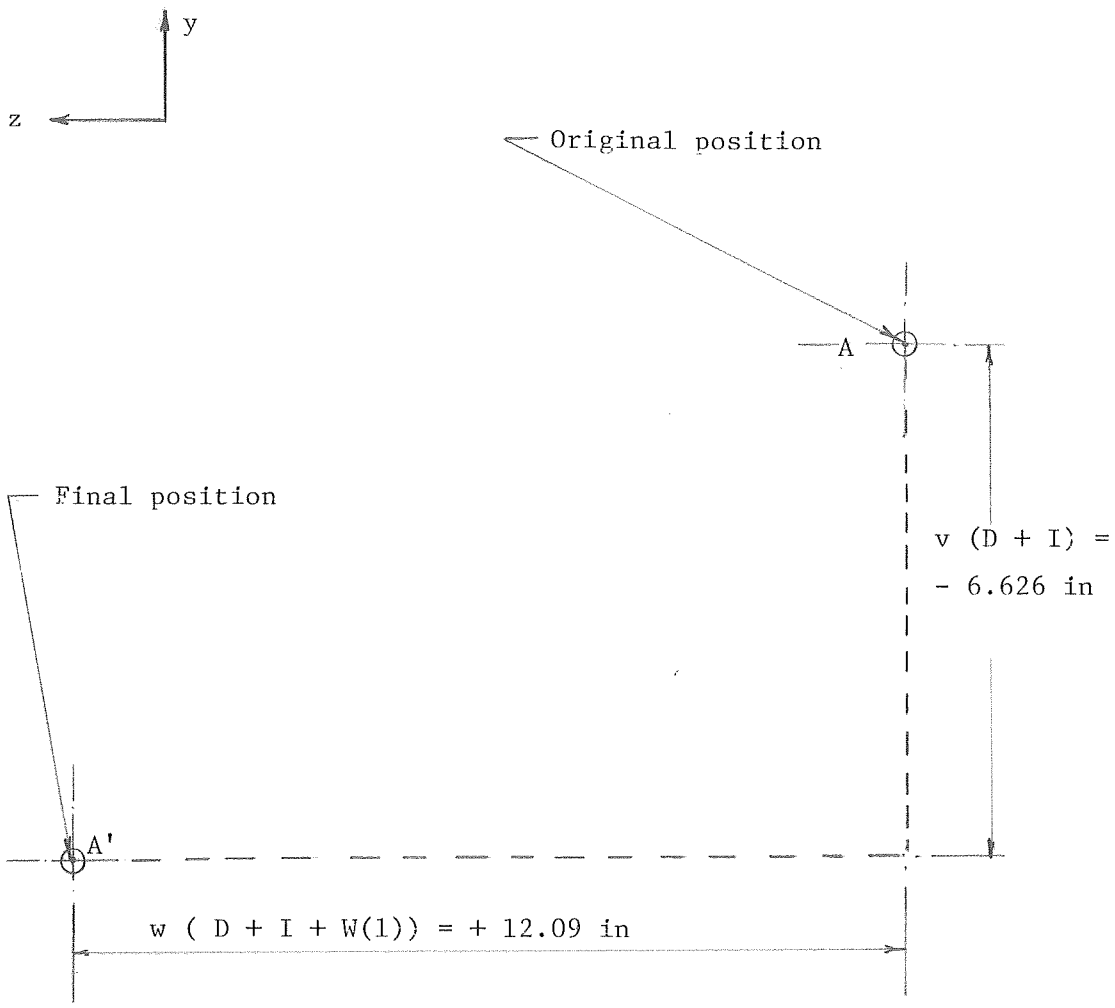

Fig. 4.9 Components of the Static Displacement for Node No. 16 (i.e. at midspan of beam)

Table 4.4

Static Forces due to D + I + W(1)
Load Combination

Elem. No.	Node No.	Axial Force (lbs)	Shear (in-pl.) (lbs)	Shear (out-of pl.)(lb)	Torsion (in-lb)	Moment (out-of-plane)	Moment (in-pl.)
1	1	-3.135E 03	2.628E 03	1.481E 03	-1.751E 04	-3.556E 05	-2.589E 05
	2	-3.135E 03	2.628E 03	1.481E 03	-1.751E 04	-2.623E 05	-9.333E 04
2	30	-3.640E 03	-2.628E 03	-2.205E 03	2.269E 04	-3.969E 05	-5.688E 04
	31	-3.640E 03	-2.628E 03	-2.205E 03	2.269E 04	-5.359E 05	-2.224E 05
3	2	-2.928E 03	2.628E 03	1.434E 03	-1.751E 04	-2.623E 05	-9.333E 04
	3	-2.928E 03	2.628E 03	1.434E 03	-1.751E 04	-1.720E 05	7.221E 04
4	29	-3.453E 03	-2.628E 03	-2.158E 03	2.269E 04	-2.610E 05	1.097E 05
	30	-3.453E 03	-2.628E 03	-2.158E 03	2.269E 04	-3.969E 05	-5.688E 04
5	3	-2.732E 03	2.628E 03	1.383E 03	-1.751E 04	-1.720E 05	7.220E 04
	4	-2.732E 03	2.628E 03	1.383E 03	-1.751E 04	-8.485E 04	2.377E 05
6	28	-3.257E 03	-2.628E 03	-2.107E 03	2.269E 04	-1.283E 05	2.742E 05
	29	-3.257E 03	-2.628E 03	-2.107E 03	2.269E 04	-2.610E 05	1.097E 05
7	4	-2.547E 03	2.628E 03	1.329E 03	-1.751E 04	-8.485E 04	2.377E 05
	5	-2.547E 03	2.628E 03	1.329E 03	-1.751E 04	-1.100E 03	4.033E 05
8	27	-3.072E 03	-2.628E 03	-2.053E 03	2.269E 04	1.101E 03	4.397E 05
	28	-3.072E 03	-2.628E 03	-2.053E 03	2.269E 04	-1.283E 05	2.742E 05
9	6	-2.628E 03	-2.371E 03	1.280E 03	1.102E 03	-4.507E 03	3.788E 05
	7	-2.628E 03	-2.371E 03	1.280E 03	1.102E 03	5.950E 04	2.603E 05
10	25	-2.628E 03	2.894E 03	-2.004E 03	1.102E 03	9.775E 04	2.652E 05
	26	-2.628E 03	2.894E 03	-2.004E 03	1.102E 03	-2.444E 03	4.100E 05
11	7	-2.628E 03	-2.221E 03	1.237E 03	1.102E 03	5.948E 04	2.603E 05
	8	-2.628E 03	-2.221E 03	1.237E 03	1.102E 03	1.337E 05	1.270E 05
12	24	-2.628E 03	2.746E 03	-1.961E 03	1.102E 03	2.154E 05	1.004E 05
	25	-2.628E 03	2.746E 03	-1.961E 03	1.102E 03	9.777E 04	2.652E 05
13	8	-2.628E 03	-2.049E 03	1.188E 03	1.102E 03	1.337E 05	1.270E 05
	9	-2.628E 03	-2.049E 03	1.188E 03	1.102E 03	2.050E 05	4.083E 03
14	23	-2.628E 03	2.574E 03	-1.911E 03	1.102E 03	3.301E 05	-5.401E 04
	24	-2.628E 03	2.574E 03	-1.911E 03	1.102E 03	2.155E 05	1.004E 05
15	9	-2.628E 03	-1.859E 03	1.133E 03	1.102E 03	2.050E 05	4.047E 03
	10	-2.628E 03	-1.859E 03	1.133E 03	1.102E 03	2.799E 05	-1.196E 05

Table 4.4 (cont'd)

Static Forces due to D + I + W(1)
Load Combination

Elem. No.	Node No.	Axial Force (lbs)	Shear (in-pl.) (lbs.)	Shear (out-of plane)	Torsion (in-lb)	Moment (out-of-plane)	Moment (in-pl.)
16	22	-2.628E 03	2.077E 03	-1.374E 03	1.102E 03	4.208E 05	-1.911E 05
	23	-2.628E 03	2.077E 03	-1.374E 03	1.102E 03	3.302E 05	-5.400E 04
17	10	-2.627E 03	-1.648E 03	1.073E 03	1.102E 03	2.798E 05	-1.186E 05
	11	-2.627E 03	-1.649E 03	1.073E 03	1.102E 03	3.506E 05	-2.273E 05
18	21	-2.628E 03	1.866E 03	-1.314E 03	1.102E 03	5.076E 05	-3.143E 05
	22	-2.628E 03	1.866E 03	-1.314E 03	1.102E 03	4.208E 05	-1.911E 05
19	11	-2.628E 03	-1.438E 03	1.013E 03	1.102E 03	3.505E 05	-2.273E 05
	12	-2.628E 03	-1.438E 03	1.013E 03	1.102E 03	4.098E 05	-3.115E 05
20	20	-2.628E 03	1.336E 03	-7.706E 02	1.102E 03	5.527E 05	-3.924E 05
	21	-2.628E 03	1.336E 03	-7.706E 02	1.102E 03	5.076E 05	-3.143E 05
21	12	-2.628E 03	-1.231E 03	9.539E 02	1.102E 03	4.098E 05	-3.115E 05
	13	-2.628E 03	-1.231E 03	9.539E 02	1.102E 03	4.656E 05	-3.835E 05
22	19	-2.629E 03	1.129E 03	-7.112E 02	1.102E 03	5.944E 05	-4.585E 05
	20	-2.628E 03	1.129E 03	-7.112E 02	1.102E 03	5.527E 05	-3.925E 05
23	13	-2.628E 03	-1.075E 03	9.073E 02	1.102E 03	4.655E 05	-3.835E 05
	14	-2.628E 03	-1.075E 03	9.073E 02	1.102E 03	4.900E 05	-4.125E 05
24	18	-2.627E 03	9.727E 02	-6.493E 02	1.103E 03	6.124E 05	-4.847E 05
	19	-2.627E 03	9.727E 02	-6.493E 02	1.103E 03	5.948E 05	-4.585E 05
25	14	-2.628E 03	-8.860E 02	8.531E 02	1.102E 03	4.900E 05	-4.125E 05
	15	-2.629E 03	-8.860E 02	8.531E 02	1.102E 03	5.514E 05	-4.763E 05
26	17	-2.628E 03	4.642E 02	-1.302E 02	1.102E 03	6.217E 05	-5.181E 05
	19	-2.628E 03	4.642E 02	-1.302E 02	1.102E 03	6.123E 05	-4.847E 05
27	15	-2.628E 03	-5.981E 02	7.713E 02	1.102E 03	5.514E 05	-4.762E 05
	16	-2.628E 03	-5.981E 02	7.713E 02	1.102E 03	6.070E 05	-5.193E 05
28	16	-2.627E 03	1.469E 01	2.063E 02	1.102E 03	6.070E 05	-5.193E 05
	17	-2.627E 03	1.469E 01	2.063E 02	1.102E 03	6.218E 05	-5.192E 05
29	5	-2.627E 03	-2.447E 03	1.301E 03	1.102E 03	-1.751E 04	4.033E 05
	6	-2.627E 03	-2.447E 03	1.301E 03	1.102E 03	-4.503E 03	3.789E 05
30	26	-2.628E 03	2.972E 03	-2.025E 03	1.102E 03	-2.435E 03	4.100E 05
	27	-2.628E 03	2.972E 03	-2.025E 03	1.102E 03	-2.269E 04	4.397E 05

The latter were obtained by simple stress analyses, using the stress resultant values.

The first point is node 16, located at the middle of the span of the beam, where the largest displacements and beam stresses were expected to occur. The second point is node 31, located at the base of the column, where a combination of bending and axial stresses are likely to control the design of the column.

The normal stresses for points 16 and 31 for different loading combinations are given in Table 4.5. It is clear that the maximum static stress occurs at the base of the column under a combination of dead plus ice plus wind loads, and is equal to 18.65 ksi. The maximum bending stress at the midspan of the beam under a combination of gravity and equivalent wind loads has been calculated as 17.30 ksi. As far as the static behavior of the structure is concerned, both of these stresses provide ample margins of safety for the structure. In particular, it is observed that the steel that is commonly used in monotube structures has a yield stress of 55 ksi. Using the AISC Specification (11), for example, this gives basic allowable stresses for circular prismatic tubular members as

(a) Gravity loads only: $F_{all} = 0.6\ F_y = 33$ ksi

(b) Gravity + Wind loads: $F_{all} = 1.33.33 = 44$ ksi

and it is seen that the allowable values are well in excess of the actual stresses. It is therefore obvious that it is not difficult to meet the strength requirements of the specifications. The current serviceability criterion is the $d^2/400$ formula; its value for the monotube structures has been commented upon and will be further discussed in Volume II (Appendix C).

TABLE 4.5
Maximum Bending Stresses (1) (KSI)

Load Combination	Midspan of Beam	At Base of Column
D	7.70	5.54
D + I	11.23	8.11
D + W	15.22	17.70
D + I + W	17.30 (2)	18.65

---

(1) Axial stresses are not included; their values are well below 1 ksi everywhere.

(2) Typically calculated with the data from Table 4.4 as

$$\frac{M}{S} = \frac{\sqrt{M_y^2 + M_z^2}}{S}$$, for point 16.

S = 46.24 in^3 = section modulus for cross section at this point on the beam; M_y = 607 k-in and M_z = 519.3 k-in for this loading case. In other words, biaxial bending is considered.

5. DYNAMIC BEHAVIOR OF MONOTUBE STRUCTURES

5.1 Description of Typical Structure

The structure that was used for the static behavior study was also used to evaluate the dynamic behavior. This facilitates a coordinated study of the static and dynamic behavior of the same structure, in order to observe the relationships between the two with respect to its response to normal loading conditions. The structure and its different structural details have been shown in Figures 4.1 to 4.4.

5.2 Modeling of the Structure

The finite element discretization that was used for the static model was also utilized to examine the dynamic behavior of the monotube structure. The original structure is shown in Figure 4.1; the FEM discretization is given in Figure 4.5.

The structure is idealized as either a plane frame or a space frame with masses lumped at the finite element nodes, depending on whether 2D or 3D modeling is to be done. The masses of the traffic-signs are lumped at the relevant nodes. In all cases, the lumped masses are assumed to have only translational degrees of freedom.

The basic finite element model with additional masses for signs is shown in Figure 5.1. The lumped masses for the bare frame are automatically generated and applied, as needed by the computer program, (23) and are therefore not shown in Figure 5.1.

5.3 Computer Program

The computer program GIFTS (23) that was used for the static analysis is also used for the dynamic evaluation. A general description of this program has been provided in Chapter 4.3.

5.3.1 Determination of natural nodes of vibration. The computer program GIFTS (23) uses the "subspace iteration method" for the computation of the eigenvalues and modes which give the natural frequencies and mode shapes. GIFTS handles the masses in lumped format in the translational directions only. For a given frame, the program generates the mass matrix for the masses of the bare frame, along with any additional lumped mass considering only the translational degrees of freedom. In this way, the program is capable of giving at the most the first ten natural frequencies and mode shapes. This is usually more than sufficient for civil engineering structures.

5.3.2 Transient response analysis. A structure subjected to time-dependent loads will have a time-dependent response. GIFTS can determine this, considering the external loads and the inertia of the

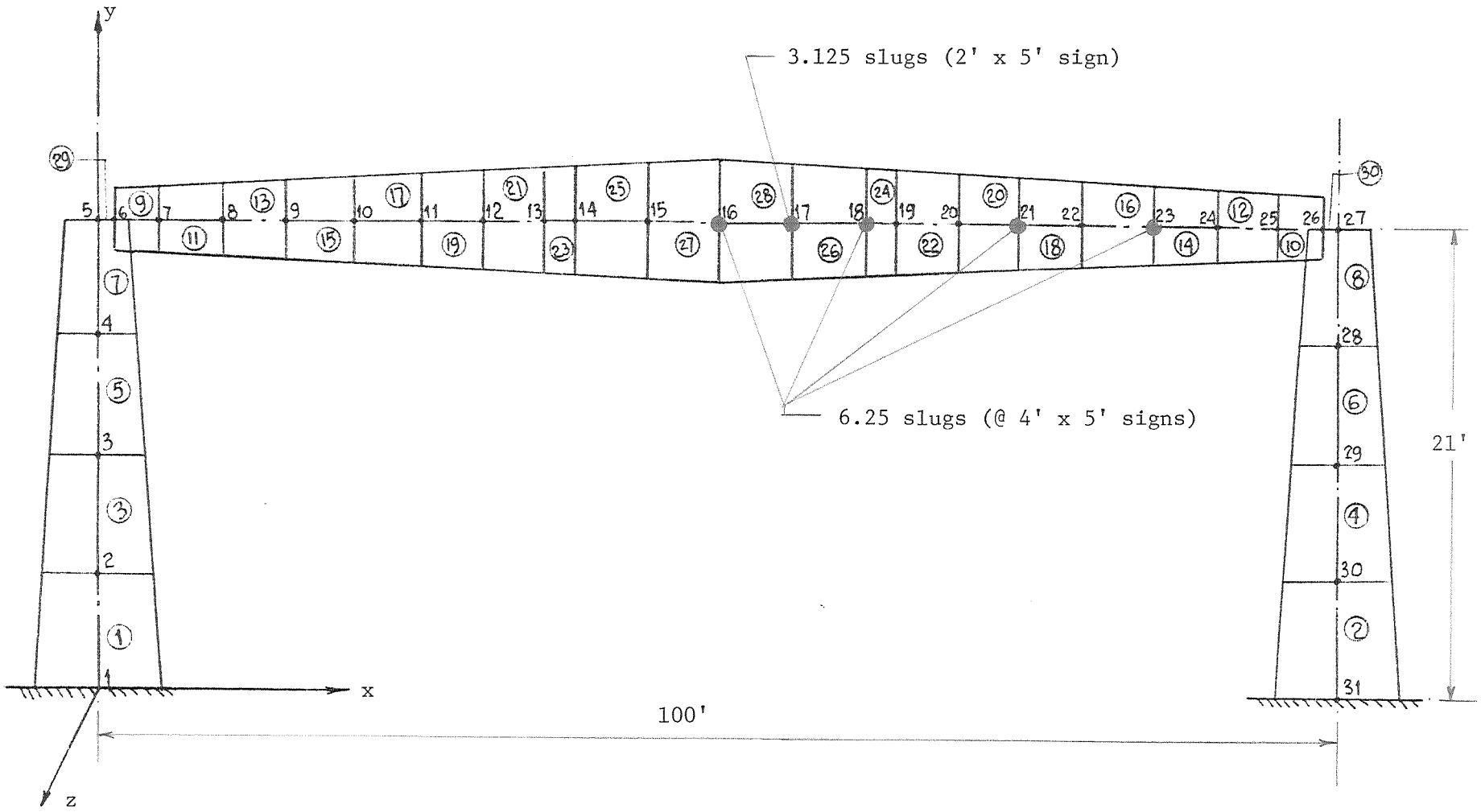

Fig. 5.1 Discretization for Dynamic Loads and Masses due to Signs

structure as well as damping forces. The transient response analysis can be performed using GIFTS through one of the five different methods. The methods are: (1) Modal Analysis, (2) Houbolt Method, (3) Newmark's Beta Method, (4) Wilson's Theta Method, and (4) Trapezoidal Rule.

The program has been used to obtain the response of the sign support structure when it is subjected to a time-dependent vortex-shedding force. This is caused by wind blowing across the plane of the frame, but the vortex-shedding occurs in-plane. A detailed discussion of the development of these loads is given in Chapter 5.4.

The computer program can compute the response of the structure under the action of the time-dependent loads at specified time steps. After obtaining the response of the structure in terms of deflections at different nodes of the finite element model, the dynamic stresses may be computed at the same time steps at which the deflections have been determined.

Modal analysis is very effective in finding the principal modes and the corresponding natural frequencies that dominate the dynamic behavior. This analysis may be performed effectively by using the first few dominant modes.

The other four methods are basically different forms of direct time integration schemes. Regarding these direct integration schemes, it can be said that the quality of the results is largely dependent upon the choice of time-step size. This depends on the dominant natural frequencies of the structure and the excitation frequency.

5.4 Loads

A stead wind blowing against a cylindrical structural member induces vibrations in the member that are perpendicular to the wind direction, due to the formation of vortices alternatively on the two sides of the member in addition to the wind itself.

The frequency Ω of the alternating vortices is determined from the equation

$$\Omega = \frac{SV}{D} \qquad (5.1)$$

where S is the non-dimensional Strouhal number, which varies with the Reynolds Number R, as illustrated in Figure 5.2 (6). V is the wind velocity and D is the diameter of the cylindrical member.

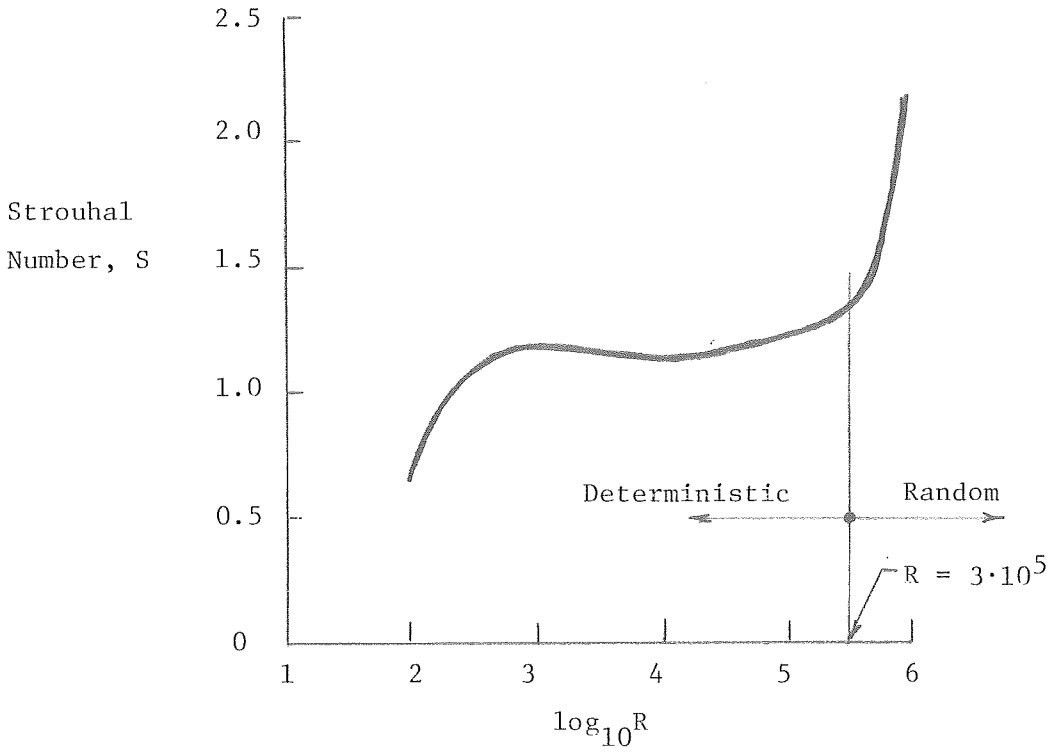

Fig. 5.2 Relationship Between Strouhal Number, S, and the logarithm of Reynolds Number, R (6).

The Reynolds Number for air is defined as

$$R = 780.5 \cdot V \cdot D \qquad (5.2)$$

where V is the wind velocity in miles per hour and D is the diameter of the cylinder in inches.

For the purpose of computing the response of an elastic system, the following two ranges of R must be considered (6):

1. For $300 < R < 3 \times 10^5$, the forcing function is sinusoidal with a deterministic frequency but a random amplitude.

2. For $R > 3 \times 10^5$, the forcing function is sinusoidal but with random frequency and random amplitude. The first range is of primary interest because most members of highway sign structures subjected to moderate wind velocities fall into this category.

Vortex shedding forces can and have been observed to cause sustained vibrations when the frequency of vortex shedding is nearly equal to the frequency of one of the natural modes of vibration of the structure (13). If the structural damping is small, as in the case of monotube structures, and if the wind remains steady, it is possible that large amplitude vibrations may develop.

For $300 < R < 3 \times 10^5$, the generally accepted expression for the alternating force is (13):

$$F(t) = \frac{1}{2} \rho V^2 A_p C_L \sin\Omega t \qquad (5.3)$$

where $F(t)$ = time dependent vortex shedding force
ρ = density of dry air
V = velocity of wind
A_p = projected area of the cylinder
C_L = force coefficient
t = time

To account for the random force amplitude, Weaver (13) has experimentally determined the root-mean-square (rms) values of C_L (denoted as $\bar{C}_L$), and using these the expression for the alternating force becomes:

$$F(t) = \frac{1}{2} \rho V^2 A_p \bar{C}_L \sin\Omega t \qquad (5.4)$$

5.4.1 Determination of F(t): Vortex shedding frequency equal to natural frequency. As an example, the vortex shedding frequency that equals the first mode natural frequency of 0.469 cps (three-dimensional) will be determined. This is an iterative procedure and is demonstrated in the following (13). It is noted that the value of the average diameter of the cylindrical members, D, has been set as 14 inches.

First Trial: V = 2 mph
From Eq. (5.2):

$$\log_{10}R = \log_{10}(780.5 \times 2 \times 14) = 4.34$$

Figure 5.2 then gives a value of S = 1.16.

From Eq. (5.1), using Ω = 0.469 cps, S = 1.16, and D = 14 inches, the value of V is obtained as:

$$V = 0.469 \times 2 \times \frac{14}{1.16}$$

$$= 2.02 \text{ mph}$$

Second Trial: V = 2.02 mph

$$\log_{10}R = \log_{10}(780.5 \times 2.02 \times 14) = 4.344$$

From the plot of S vs. $\log_{10}R$, the value of S is obtained as 1.16. Confirming that the iteration scheme has converged, using Ω = 0.469 cps, S = 1.16, and D = 14 inches, the value of V is found from Eq. (5.1) as 2.02 mph.

This trial therefore has given a wind velocity of 2.02 mph that will produce vortex shedding with a frequency equal to 0.469 cps; i.e., matching the natural frequency of the first 3D mode of structure. The forcing function, F(t), is determined from Eq. (5.4):

$$F(t) = 1/2\rho V^2 A_p \overline{C_L} \sin \Omega t$$

where ρ = 0.002378 slug/ft^3

V = 2.02 mph = 2.963 ft/sec

A_p = projected area (ft^2) for a node of the finite element model (see Fig. 5.1)

$\overline{C_L} = 1.0$

$\Omega = 2\,\pi(0.4692)$ rad/sec

Hence: $F(t) = 1/2\ (.002378)\cdot(2.963)^2\cdot A_p\cdot(1.0)\cdot\sin[2\pi(0.4692)t]$

$$F(t) = 0.01044\cdot A_p\cdot\sin[2\ \ (0.4692)t] \qquad (5.5)$$

This equation for F(t) can be used to find the individual nodal point loads due to the vortex shedding. It is important to note that for nodes on the column member, F(t) acts horizontally in-plane, whereas for the nodes on the beam member, F(t) acts vertically in-plane. Again, the vortex shedding takes place in a plane perpendicular to the wind direction and the longitudinal axis of the individual member.

5.4.2 Determination of F(t) for any wind velocity. In order to study the response at any wind velocity for Reynolds Numbers in the range of $300 < R < 3 \times 10^5$, the forcing function F(t) can be determined as shown in the following example.

As an example, a wind speed of V = 25 mph is considered. Hence, with a tube diameter of 14", this gives $\log_{10}R = \log_{10}(780.5 \times 25 \times 14) = 5.44$. From the plot of S vs. $\log_{10}R$ (see Fig. 5.2), the value of S is obtained as 1.32143.

From Eq. (5.1), using S = 1.32143, V = 25 mph = 439.99 in/sec, and D = 14 in, the value of Ω is found as:

$$\Omega = 1.32143 \times \frac{439.99}{14} = 6.61 \text{ cps.}$$

F(t) is now determined from Eq. (5.4) as

$$F(t) = 1/2\ (.002378)\ (36.67)^2\ A_p\ (1.0)\ \sin\ [2\pi\ (6.6097)t]$$

$$F(t) = 1.599\ A_p\ \sin\ [2\pi(6.6097)t]$$

where 36.67 is the wind speed in ft/sec. The nodal forces can now be found for each individual node, given the corresponding value of A_p.

5.5 Dynamic Behavior: Free Vibration of the Monotube Structure

5.5.1 General Introduction. The free natural vibration characteristics of the structure are representative of the dynamic behavior of the structure without the influence of any external load or forcing function, as the dynamic load is often called. These properties can be determined by an iterative technique, such as subspace iteration, and the structure can be treated as a distributed or lumped mass system. The

former mass distribution approach gives a structure with an infinite number of degrees of freedom; the latter, which has been used to analyze the monotube sign structure, has a number of degrees of freedom that can be given as

$$(NDF) = (NP) \cdot (NFP) - (NFP)_S \qquad (5.6)$$

where NP = number of nodal points in the structure, NFP = number of degrees of freedom at each nodal point, and $(NFP)_S$ = number of suppressed degrees of freedom. The value of NFP, therefore, takes into account whether the analysis has been based on a three- or a two-dimensional representation of the structure.

A number of studies have described the numerical procedures that can be used to obtain the free vibration characteristics of a structure; the book by Clough and Penzien (24) represents an up-to-date and practical reference. The discretization of the monotube structure is described in detail in Chapter 4.2; the numerical technique that has been used to arrive at the natural dynamic properties is described in section 4 of this chapter.

The natural vibration characteristics of a structure are particularly important when it is being subjected to a set of dynamic loads. The frequencies of the loads and those of the bare structure may be such that the actual response is a magnification of the natural vibrations. In the most unfavorable case, there is agreement between the loading frequency and that of one or more of the natural vibration modes, such that the combined effect is a structure that vibrates with ever-increasing deflections. This constitutes resonance, and is a dynamic failure criterion for the structure.

In theory, the attainment of resonance is possible, and there are a few recorded instances of actual structural failures where resonance has at least played a certain part. The celebrated failure of the Tacoma-Narrows Bridge is one such extreme example; another case is that of the wind-induced vibrations known as flutter that can be encountered in some flight structures or others where the mass-to-stiffness ratio is very low. However, under realistic conditions the resonance phenomenon is one of mathematical importance only, due to the inherent damping of the structure.

It has been pointed out that in the analysis of the single span monotube structure, the amount of damping has been assumed to be equal to zero. This is a conservative assumption insofar as the structural response to forced vibration is concerned, and must be borne in mind when the forced vibration properties are presented. These data will be discussed in detail in section 6 of this chapter.

As will be shown, complete two- and three-dimensional vibration analyses have been carried out for the structure. With a total of 31 nodal points in the frame, the resulting number of degrees of freedom will be very large. However, Clough and Penzien (24) and others have observed that for most civil engineering structures only the first few modes of vibration are practically significant. For that reason, it was decided to determine the properties only of the first 10 natural modes of vibration of the monotube structures for each of the 3D and 2D analysis schemes. It will be shown that this is well in excess of what is useful; the first five modes of vibration generally dominate the response of these structures.

5.5.2 Natural Frequencies and Modes. Table 5.1 gives the natural frequencies and the natural periods for the first 10 modes of the basic monotube structure, including 2D as well as 3D data. It is emphasized that the response for the 2D-case represents x- and y-components only, since the out-of-plane motion has been suppressed. Figure 5.3 shows the front elevation view of the 2D mode-shape for Mode 1 of the structure, and Figures 5.4 (a) to (d) give the isometric and three planar views of the 3D mode-shape for Mode 1.

The data in Table 5.1 show that the following 2D and 3D modes have identical frequencies/periods:

$$f_1\ (2D) = f_2\ (3D)$$
$$f_2\ (2D) = f_3\ (3D)$$
$$f_3\ (2D) = f_5\ (3D)$$
$$f_4\ (2D) = f_8\ (3D)$$
$$f_5\ (2D) = f_{10}\ (3D)$$

Since the 2D modes are all in-plane, the above indicates that the 3D modes f_2, f_3, f_5, f_8 and f_{10} are dominated by in-plane behavior. At the same time, the first 3D mode is an out-of-plane one that is independent of in-plane properties, and is prompted by the small out-of-plane stiffness of the beam-to-column connection.

The above data and those in Table 5.1 give one of the reasons why it eventually was decided to propose design recommendations based on independent, individual analyses of the structure in the in-plane and out-of-plane directions. Due to the static gravity loads that act on the structure, along with the in-plane vortex shedding (i.e., dynamic effects of the wind load, the in-plane loading conditions and response will govern the overall structure. However, a static out-of-plane evaluation of the beam member subjected to wind loads is also necessary. It is shown that this can be accomplished by a simple, independent check of the bending stress and the deflection produced by the static equivalent of the wind load.

TABLE 5.1
Natural Frequencies and Period for Monotube Structure*

	Natural Frequency (cps)		Natural Period (sec.)	
Mode	2D	3D	2D	3D
1	0.783	0.47	1.28	2.13
2	1.494	0.783	0.67	1.28
3	3.033	1.494	0.33	0.67
4	6.377	1.91	0.157	0.524
5	10.15	3.033	0.099	0.33
6	15.61	4.083	0.064	0.245
7	23.65	6.241	0.042	0.16
8	38.28	6.377	0.026	0.157
9	39.9	9.004	0.025	0.111
10	44.3	10.15	0.023	0.099

* Frequencies and periods are related as f = 1/T.

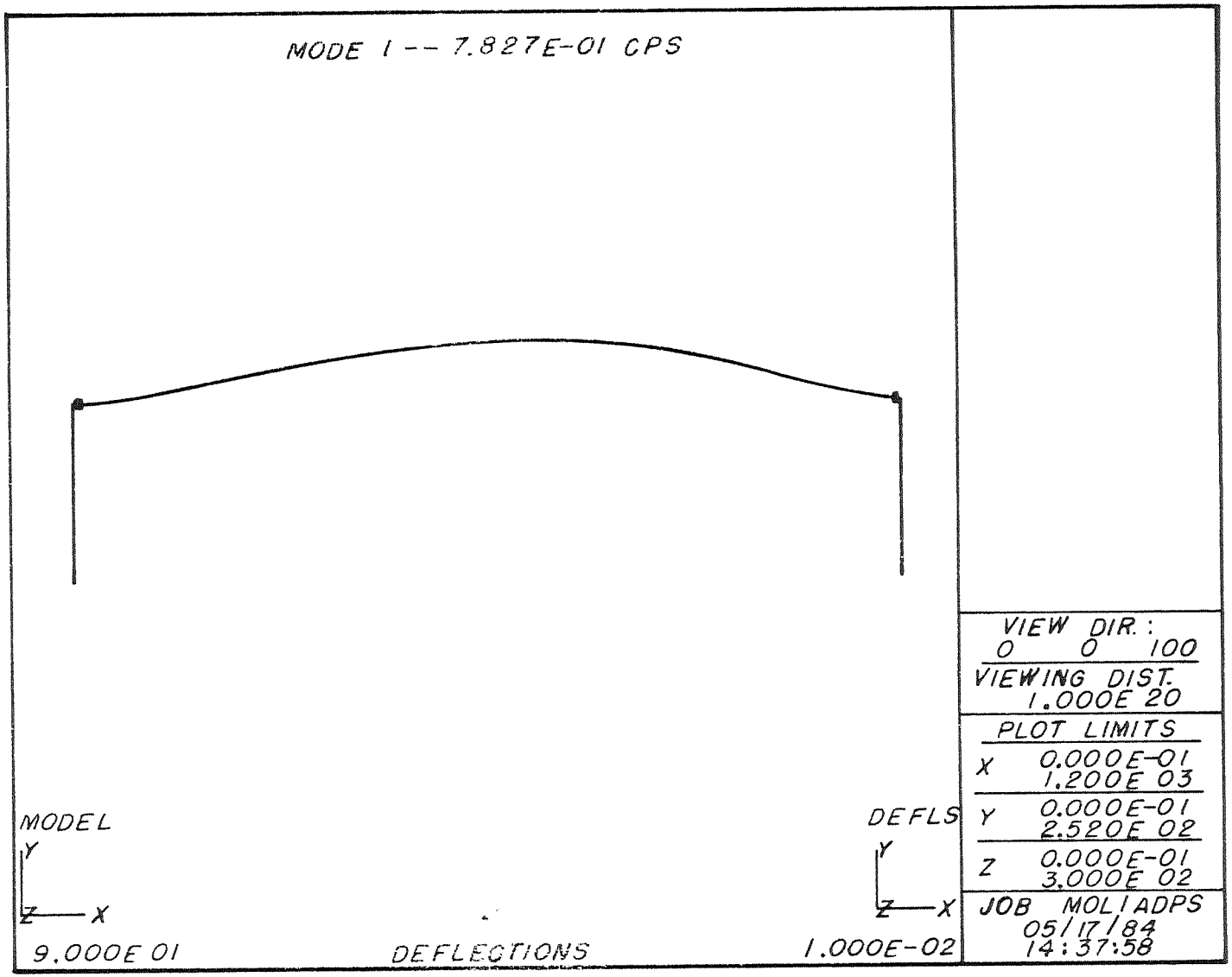

Fig. 5.3 x-y-elevation View of Mode 1 for 2D Natural Vibration

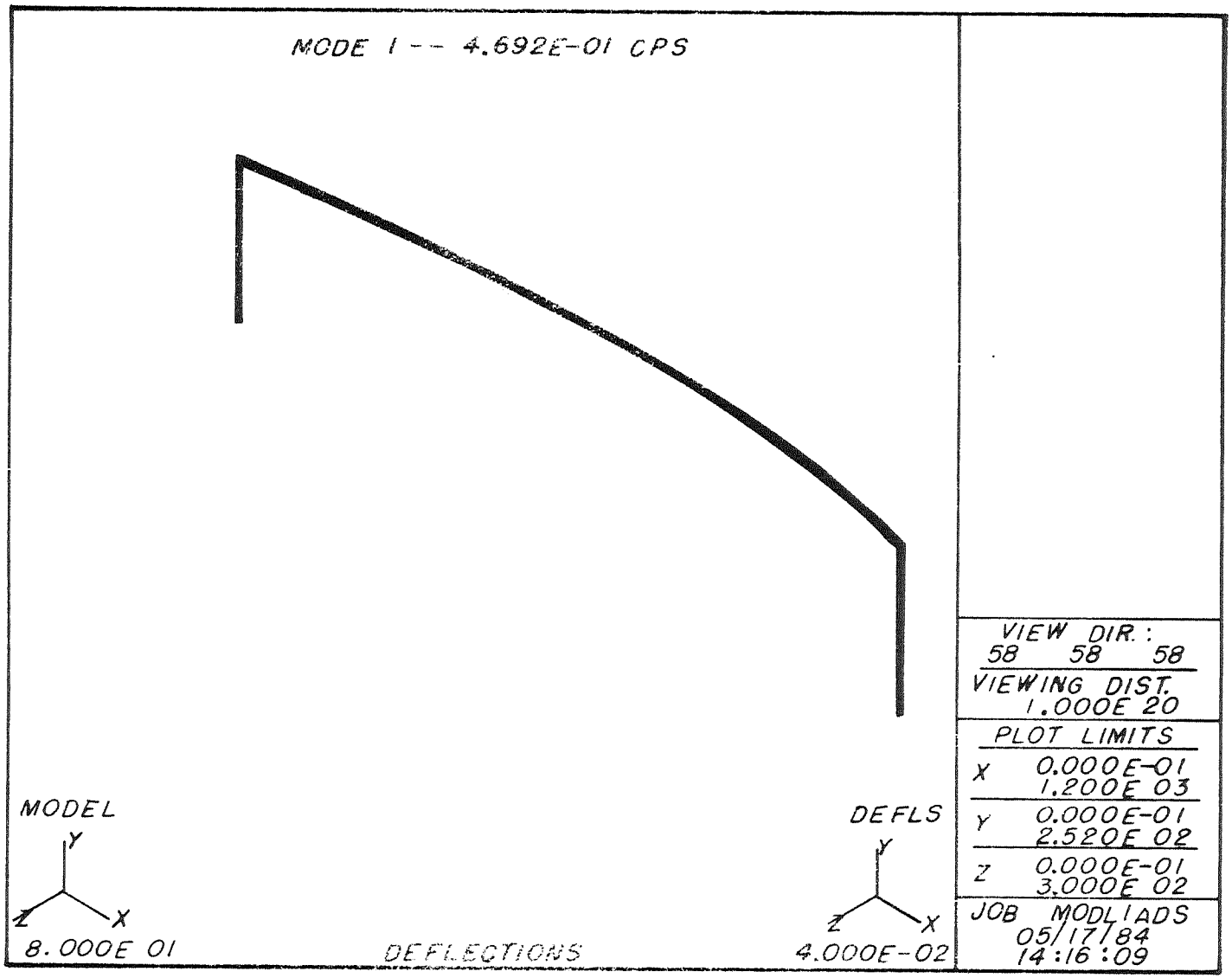

Fig. 5.4 (a) Isometric View of Mode 1 for 3D Natural Vibration

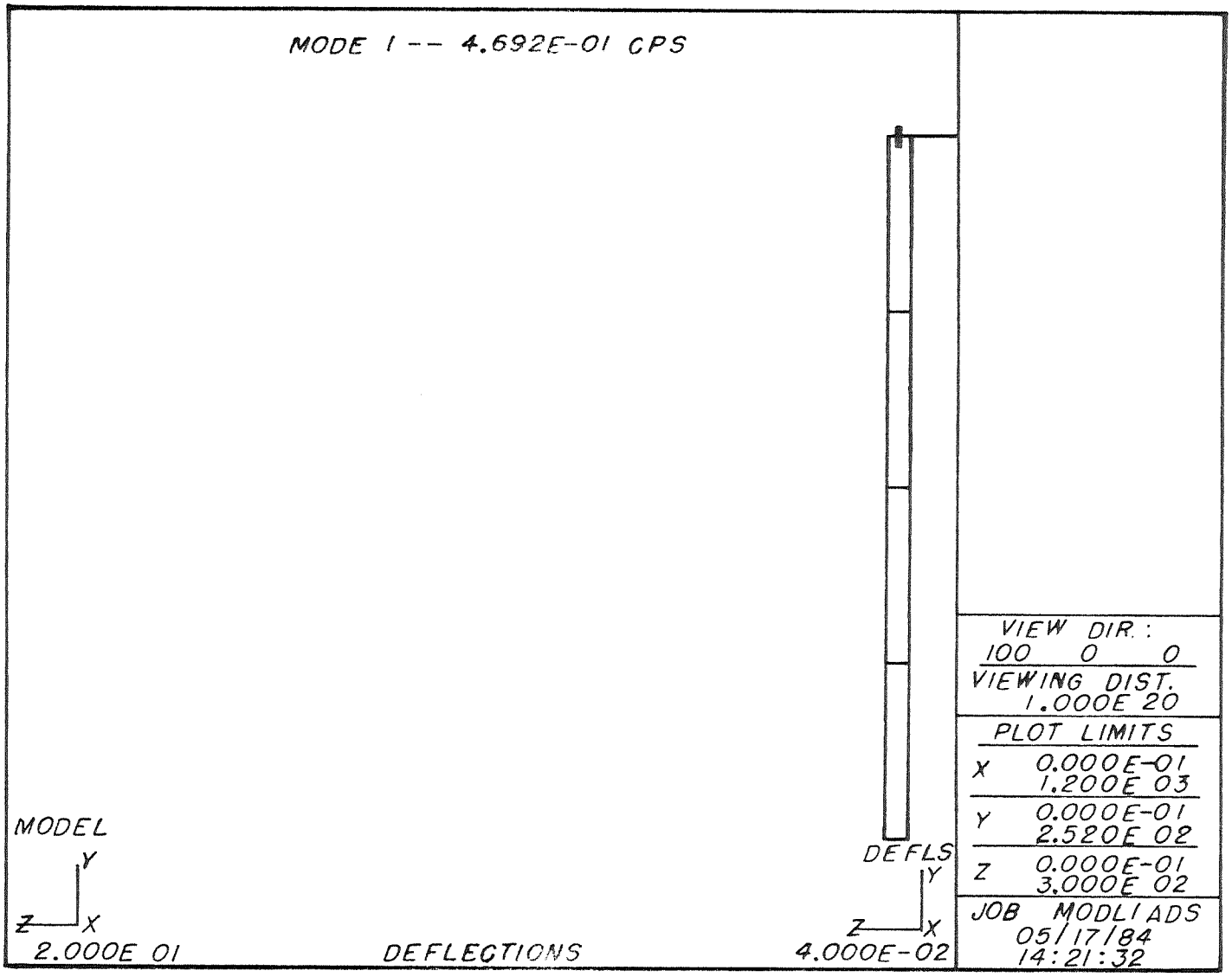

Fig. 5.4 (b) z-y-elevation View of Mode 1 for 3D Natural Vibration

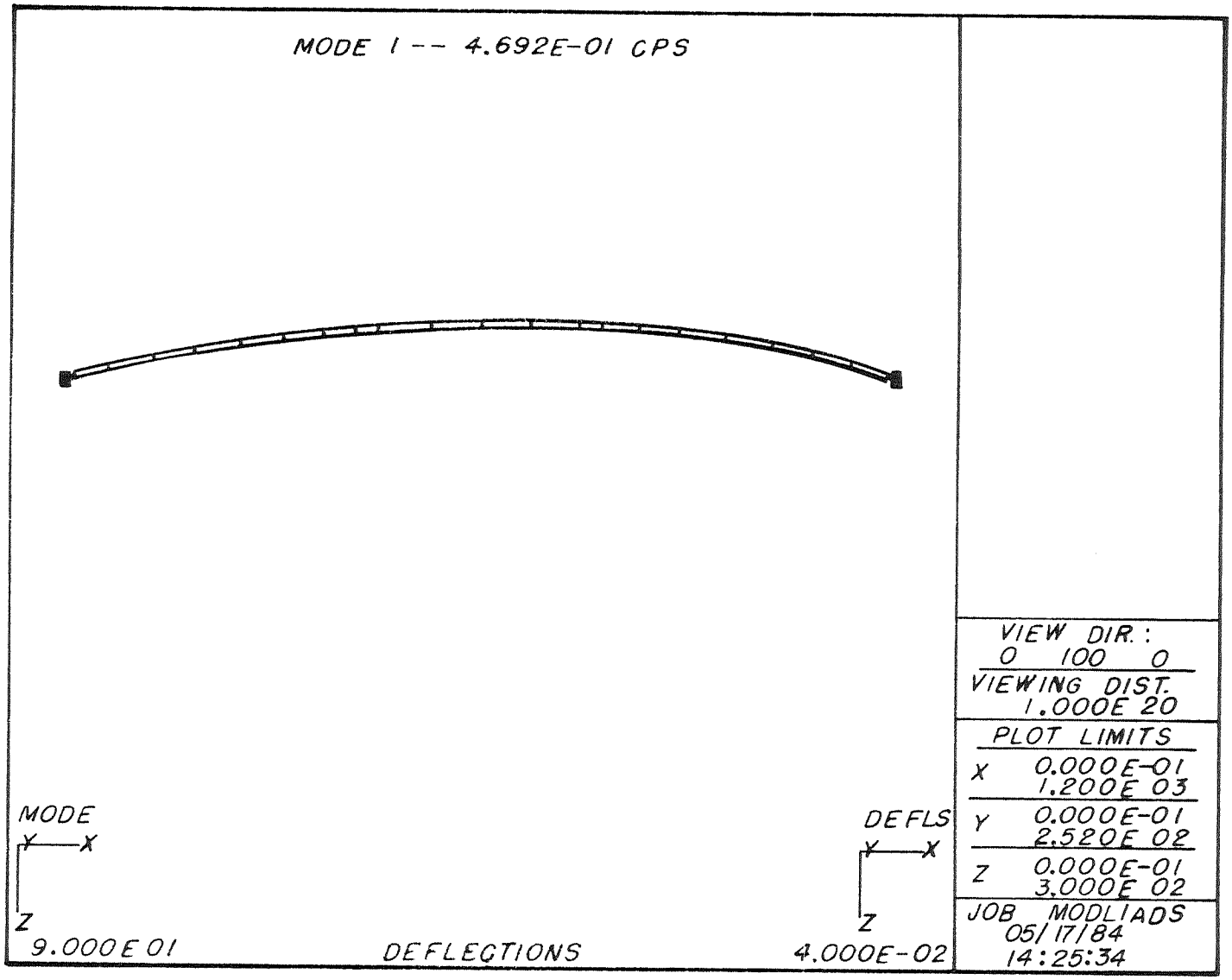

Fig. 5.4 (c) x-z-plan View of Mode 1 for 3D Natural Vibration

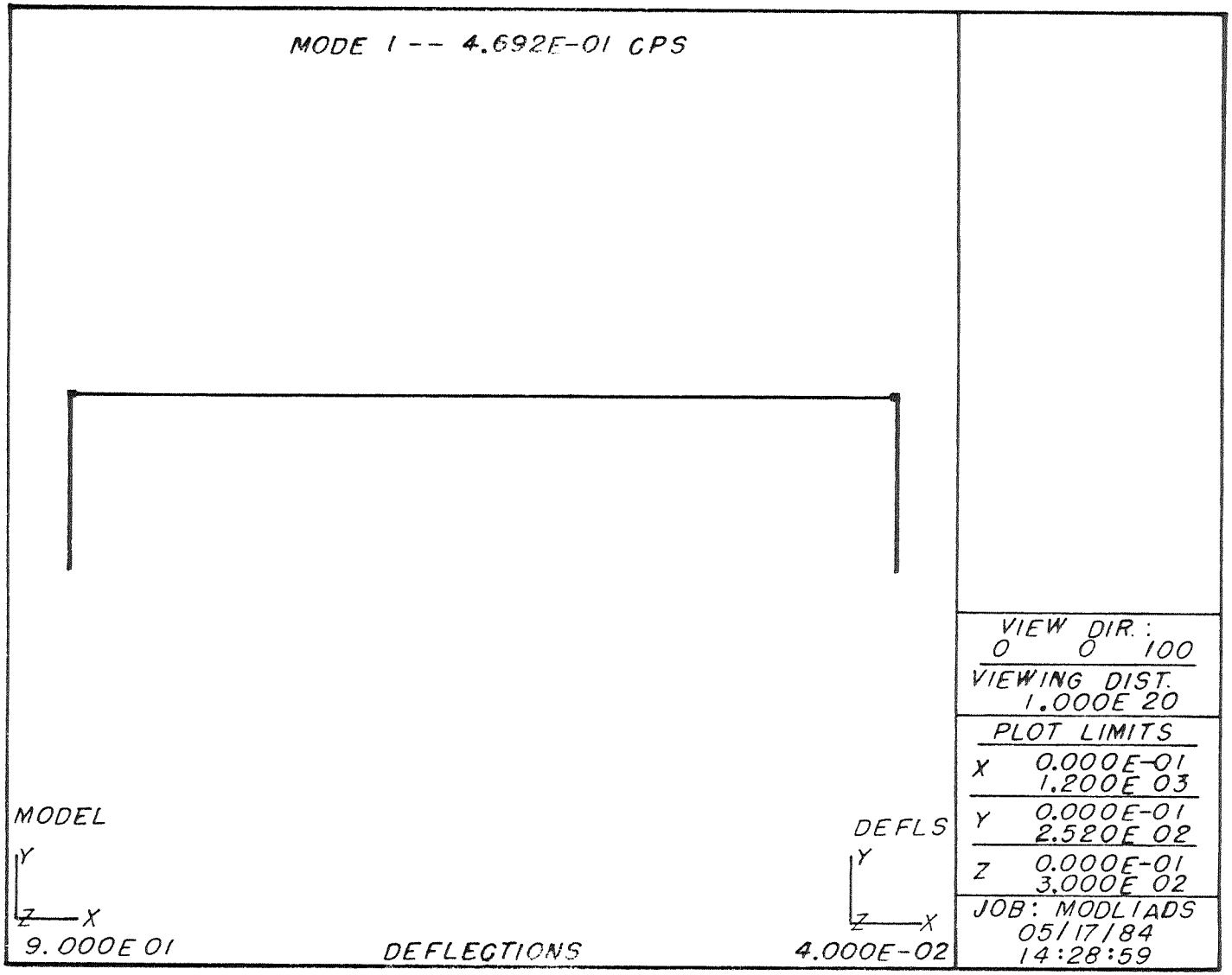

Fig. 5.4 (d) x-y-elevation View of Mode 1 for 3D Natural Vibration

The mode-shape data that were used to plot the displaced frame configurations of Figures 5.3 and 5.4 are given in Appendix A of this report, as Tables A.1 and A.11, respectively. Appendix A also gives the complete mode-shape data for the other 2D and 3D natural modes of vibration. It is emphasized that the displacements, for example, that are given in these tables, do not represent actual deflections, since the natural modes of vibration are not associated with any load. Rather, the displacements are numbers that reflect relative positions of the nodes on the deformed structure. In other words, the natural mode-shapes are used to establish the governing shapes of the vibrating structure, and to correlate these with the behavior that results when dynamic loads are applied.

5.6 Dynamic Behavior: Forced Vibration of the Monotube Structure

5.6.1 General Introduction. A detailed description of the wind loads that act on the structure has been given in Chapter 5.4, including the method that is used to determine the characteristics of the vortex shedding forces. As explained earlier, the latter produce dynamic loads that act at each node in the in-plane direction perpendicular to the longitudinal axis of the member and the direction of the wind. That is, these forces act in the vertical direction for the beam and in the horizontal direction for the columns. The vortex shedding forces therefore produce deflections that are additive to those that result from the gravity loads. In addition, careful consideration must be given to the possibility of structural resonance, as explained in Chapter 5.5.1. The determination of the wind speeds that may produce such behavior is explained in Chapter 5.4.

It is also important to note that due to the change from deterministic to random vortex-shedding behavior for Reynolds Numbers larger than 3.10^5, this study has not dealt with wind speeds larger than those corresponding to $R = 3.10^5$ for the diameters of the members of these monotube structures. This R-value reflects wind speeds of approximately 27 to 29 mph. Although actual wind speeds may exceed this value for some length of time, it is not warranted to extrapolate the deterministic model into the random behavior range. The numerical results that will be obtained if this is done are not reliable. However, as will be demonstrated by the results, realistic and practically useful data are obtained for the deterministic wind speed range.

The influence and magnitude of drag forces which act in the same direction as the wind have not been considered in this work. Due to the tubular shape of the member cross sections of the monotube structure, it is anticipated that the drag forces will be small. Furthermore, very limited data are available on the dynamic properties of these forces.

As will be seen in the presentation of the results, a choice had to be made for the length of time that the wind would be blowing at a constant speed. A duration of 32 seconds was chosen as a large multiple (approximately 16) of the longest natural period of the structure. Table 5.1 indicates that the latter is 2.13 seconds, pertaining to the first 3D mode.

It is noted that a constant wind speed duration of 32 seconds is very long, since the wind tends to gust and therefore only attain specific velocities for short periods of time. However, assuming such a long duration is conservative, especially when it comes to evaluating the resonance response. This will be discussed in detail in Chapters 5.6.2, and 6.

In the initial phase of the forced vibration analysis a numerical integration scheme was utilized to determine the response of the structure. However, due to an inherent numerical round-off error (also called numerical damping) that can only be improved upon by using very small time-steps, this computation technique was discarded in favor of modal superposition. It is noted that the latter approach is the one most commonly adopted for typical structural engineering dynamic problems.

5.6.2 Dynamic Response Due to Vortex-Shedding. The dynamic response of the monotube structures has been determined for the full range of deterministic wind speeds as outlined in Chapters 5.4 and 5.6.1. In addition to obtaining the vibration data for wind speeds where the natural and vortex shedding frequencies match, complete data have been developed for a large number of velocities. Some of the results that are presented in the following are but an example of what has been done, such as the magnitudes of nodal loads for a given wind speed and the displacement-vs-time relationships (displacement histories) for certain points in the structure. Similar data have been developed for all velocities, but only the essence of the results have been presented. That is, the relationship between the maximum in-plane displacement due to vortex shedding and the corresponding wind speed is the most useful output as far as design evaluations are concerned.

Using a mid-range wind velocity of 15 mph as an example, Figure 5.5 shows the monotube structure with the individual vortex shedding loads applied at each nodal point. Additional masses are applied at the nodes where the traffic signs are attached, as indicated. The loads are computed in accordance with the procedure that is detailed in Chapter 5.4.2. Thus, the wind speed of 15 mph corresponds to a vortex shedding frequency of 3.787 cps. Using Eq. (5.4) with $C_L = 1.0$, $\rho = 0.002378$ slugs/ft^3 and V = 15 mph = 22.0 ft/sec, this gives a general expression for the vortex shedding nodal point load of:

$$F(t) = P_{VS} = 1/2\ 0.002378\ (22)^2\ A_p\ 1\ \sin\ (2\pi \cdot 3.787)t$$

or:

$$P_{VS} = A_p \cdot 0.5755 \cdot \sin(23.78t)$$

A_p is the magnitude of the projected tributary area for any node, the forces given in Figure 5.5 reflect the actual A_p -values.

Figure 5.6 shows the displacement histories for four important points on the structure, as follows:

Nodal Point 16: Midspan of beam

Nodal Point 18: Approximately one-third of the distance between midspan and end of beam (see Figure 4.5)

Nodal Point 23: Approximately two-thirds of the distance between midspan and end of beam (see Figure 4.5)

Nodal Point 27: Top of column

These nodal points include the single most important one as far as deflections are concerned, namely, at midspan. The other two beam nodal points were included for direct comparison with midspan, as well as to give an indication of the influence of the beam-to-column connection.

The displacement histories for Points 16, 18 and 23 reflect vertical (in-plane) deflections of these points in relation to time, and the displacement history for Point 27 gives horizontal (in-plane) movement in relation to time. The maximum vertical deflection (at Point 16) equals approximately 0.2 inches; it occurs first after about 6 seconds of load duration and reoccurs roughly every 2 seconds. The response is stable, i.e., the maximum deflection does not increase with time.

As expected, the maximum horizontal deflection (at Point 27) is one order of magnitude smaller than the vertical one. It reaches a value of 0.01 inches after approximately 6 seconds, and then occurs under stable conditions every 10 to 15 seconds thereafter. It is clear that the structural significance of the horizontal in-plane deflections is limited; the only aspect of the behavior that might be affected by this may be the fatigue response of some of the structural details (beam-to-column connection; column base). However, this is a topic that is beyond the scope of this project and cannot be further evaluated here.

The maximum vertical deflection due to the dynamic load must be considered in relation to the value of the maximum static one at the

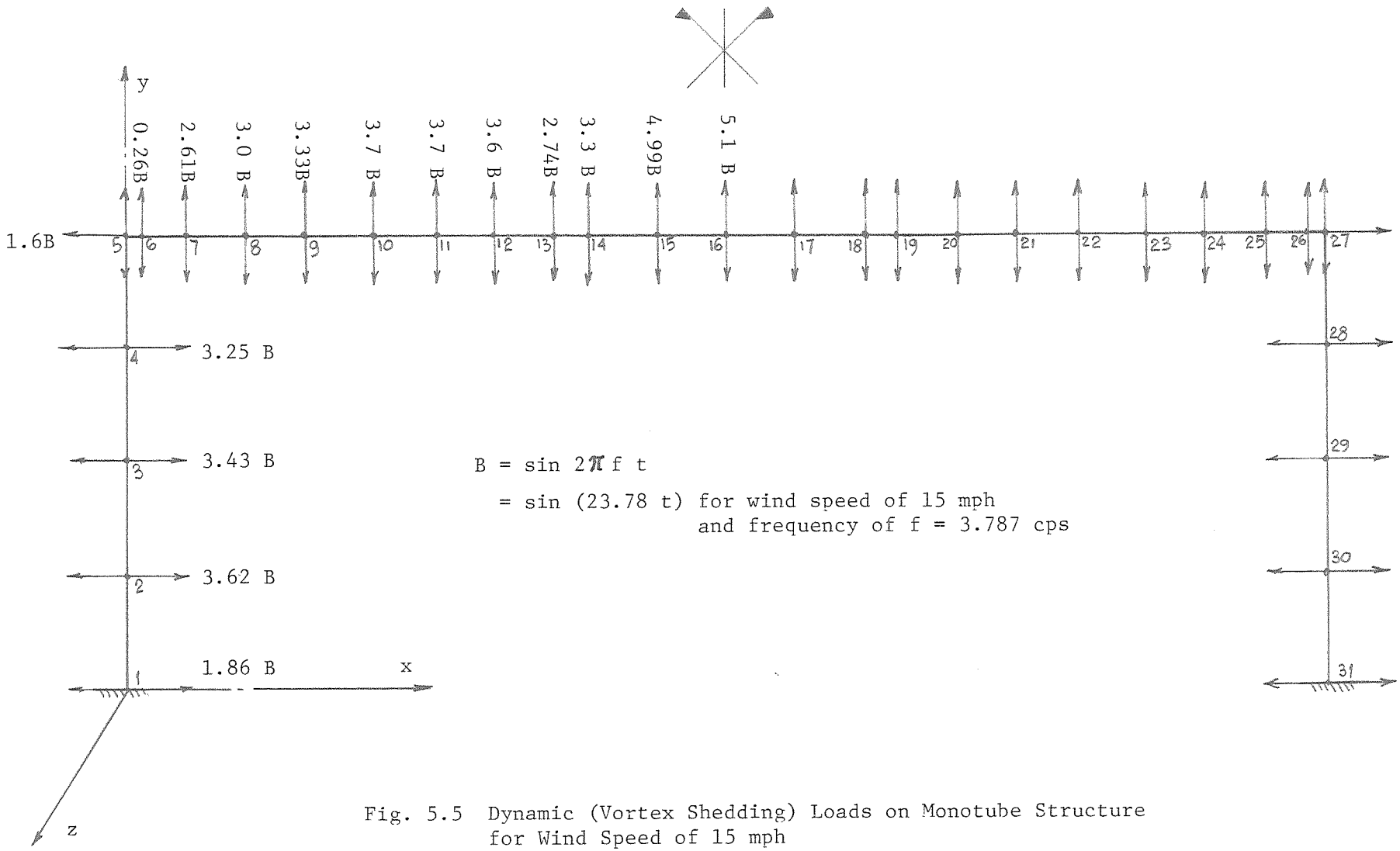

Fig. 5.5 Dynamic (Vortex Shedding) Loads on Monotube Structure for Wind Speed of 15 mph

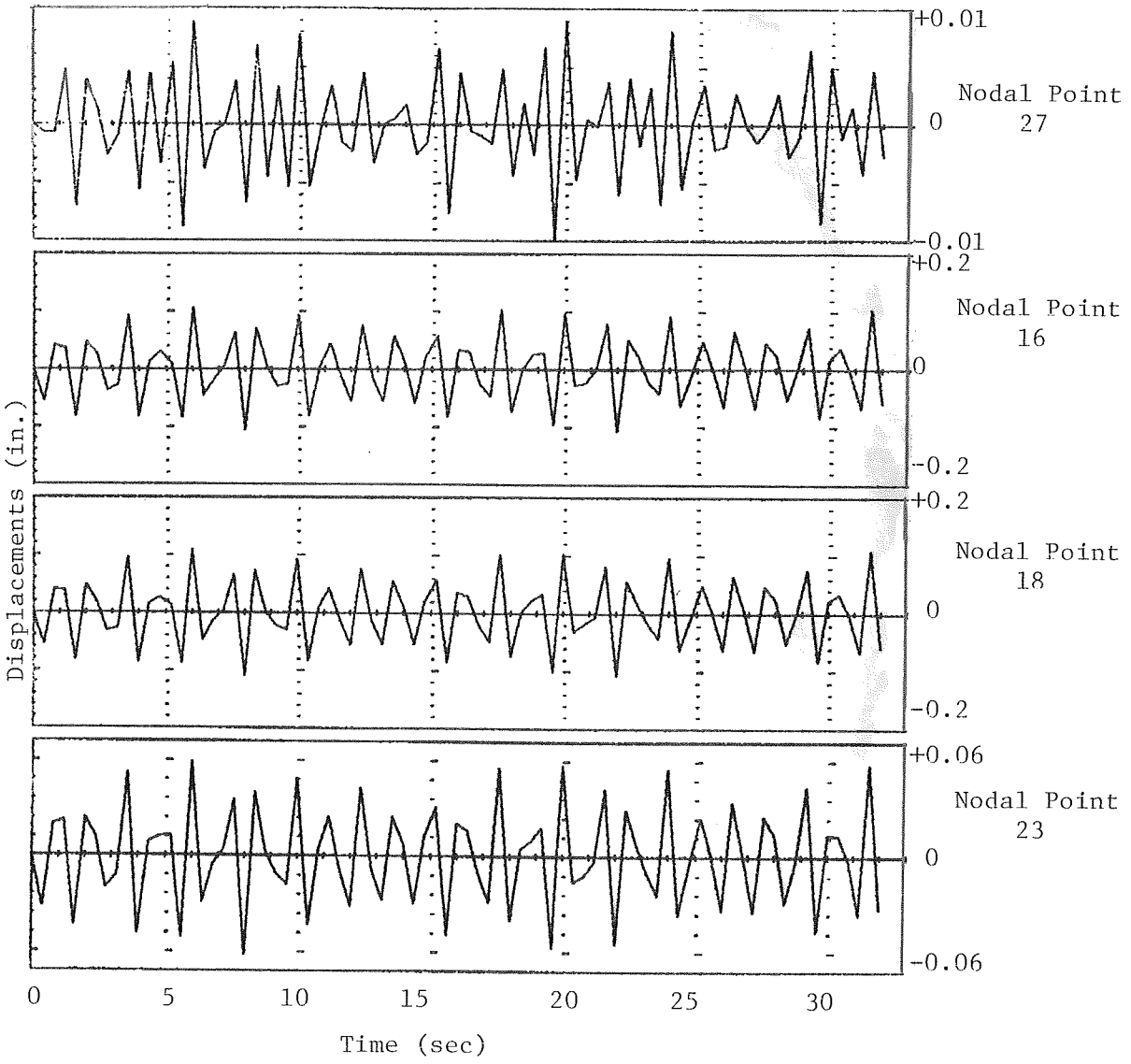

Note: For nodal point 27, the horizontal displacement is shown; for nodal points 16, 18, and 23, vertical displacements are shown.

Fig. 5.6 Displacement Histories for Nodal Points 16, 18, 23 and 27, due to a Wind Speed of 15 mph.

same point. The static displacements are given in Chapter 4; for comparison they are repeated here:

Dead Load:	Δ_{SD} = 4.56 in.
(Dead + Ice) Load:	Δ_{SG} = 6.63 in.
Dynamic (Vortex-Shedding) Load	Δ_d = 0.2 in.

The increase of the deflection due to the dynamic effect is therefore less than 5% for both dead and (dead + ice) loads. Since the allowable stresses (11, 12) are increased by one-third for the load cases that incorporate wind, it is obvious that gravity load will govern the in-plane design. This is amplified by the dynamic stress increases of 0.17 ksi and 0.22 ksi at the column base and at beam midspan, respectively.

The statically equivalent out-of-plane deflection of the beam for a wind speed of 15 mph is computed as shown in Chapter 4, namely:

$$\Delta_h\ (v = 15) \simeq \Delta_h(v = 70)\ (\frac{15}{70})^2$$

which becomes:

$$\Delta_h\ (v = 15) \simeq 0.56 \text{ in.}$$

where it is recalled that $\Delta_h\ (v = 70) = 12.09$ inches. For this wind speed the gravity load combination therefore will govern.

5.7 Correlation of Wind Speed and Maximum Amplitude

Figure 5.7 shows the relationship between the maximum dynamic vertical deflection (at Point 16) and the wind speed for the complete deterministic velocity range. Peaks are reached for velocities of 3.31 mph, 6.2 mph and 12.13 mph, corresponding to the natural frequencies for the first three 2D-modes. The maximum value of 0.3 inches occurs for the first mode; it is insignificant in comparison with the static deflections.

Large deflections appear to take place for wind speeds around 16.2 to 17.0 mph, as well as for the range of 21.0 to 23.0 mph. The peaks do not correspond to any natural frequency of the structure, but do show the tendency towards resonance for these wind speed ranges. The implications of these numbers will be explored in full in Chapters 6 and 7. However, it is emphasized here that the ranges of velocities for which resonance appears to be taking place are very narrow. At the same time, the data in Figure 5.7 have been based on a sustained wind duration of 32 seconds which is of limited practical value. It is also recalled that it has been assumed that the structure possesses no damping capability. In consequence, although large deflections are

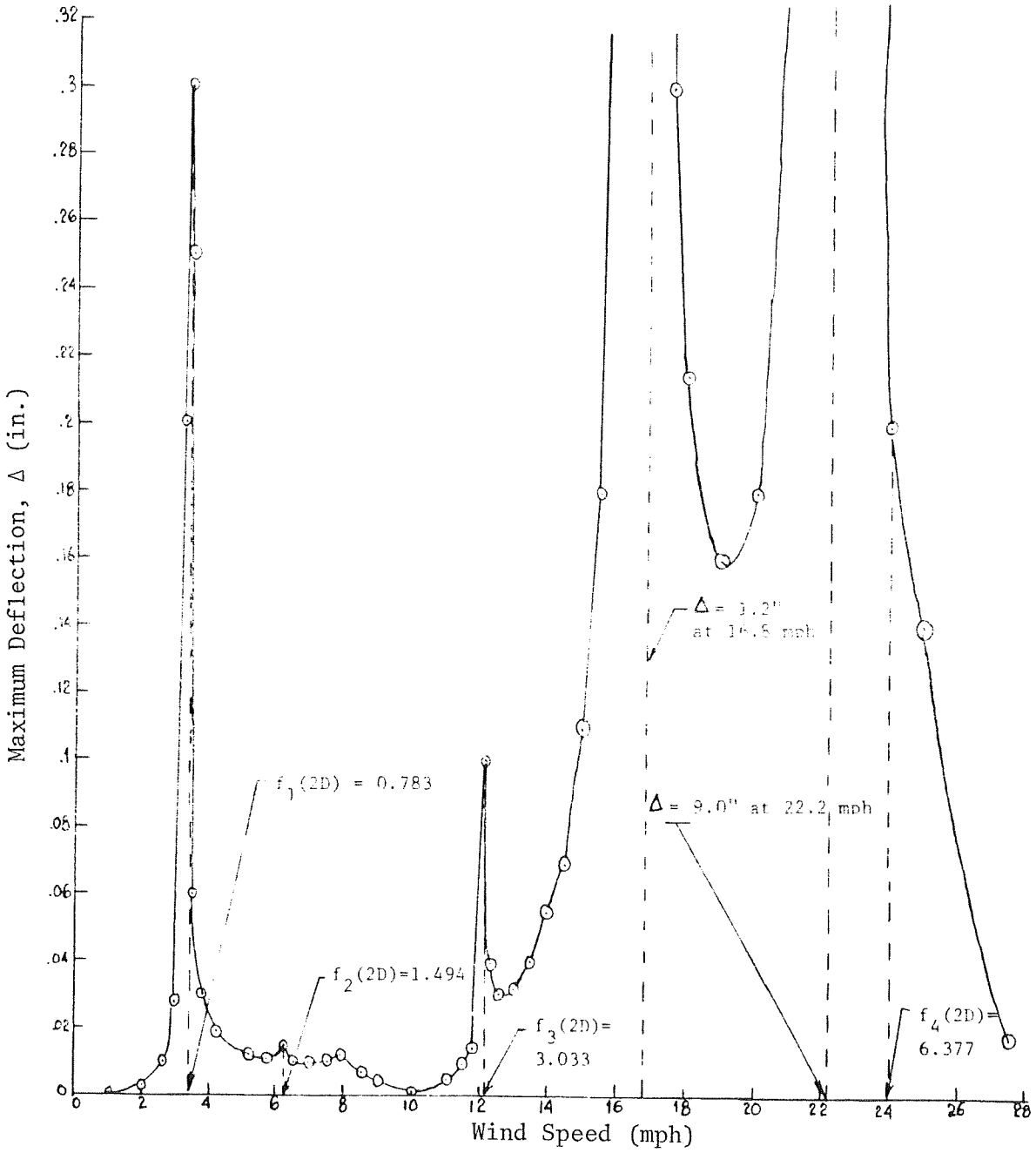

Fig. 5.7 Maximum Vertical Dynamic Deflections at Midspan of Beam for Different Wind Speeds

indicated for certain wind speeds, their practical impact is questionable.

It is also noted that at the highest wind velocity where resonance appears, i.e., V 22 mph, the statically equivalent out-of-plane deflection is found as

$$\Delta_h\ (v = 22) \simeq 12.09 \cdot \left(\frac{22}{70}\right)^2 = 1.19 \text{ in.}$$

The deflection-to-span ratio for this value is approximately 1/1000; hence, its influence on the stresses in the structure, for example, is very small.

Further evaluations of the above findings are presented in Chapter 6.